Treball de Fi de Màster

Màster universitari en Enginyeria Industrial

SMALL-SCALE PASTEURIZATION PLANT: MODELLING FOR REAL-TIME CONTROL

Autor: Sandra Terradellas Balaguer
Director/s: Dr. Carlos Ocampo Martínez
Dr. Sebastian Tornil Sin

Convocatòria: Octubre 2016

Escola Tècnica Superior
d'Enginyeria Industrial de Barcelona

Abstract

The pasteurization process is one of the most common treatments in the food industries in order to eliminate harmful pathogenic and spoilage microorganism. The process consists in maintaining a high temperature stablished during a short period of time (HTST).

Most of the pasteurization plants are controlled by tradicional PID (Proportionas-Integral-Derivative). Much effort has been made to develop advanced controllers. However, an accurate model that describes the system is required. The main of the present project is to develop a dynamical model for a pasteurization plant for a real-time control. Experimental plant consists in a small-scale pasteurization plant PCT23 MKII completely monitorized owned by the enterprise Armfield.

The first task refers to modelling the different elements of the plant. Each one is modelled using the physical principles resulting a nonlinear model. Different parameters of the proposed model are later estimated by experimental data. Finally, the complete model is validated by new experimental data. Linear parameter-varying (LPV) model represents a class of non-linear systems that can be controlled using powerful linear-like techniques. As a nonlinear model is proposed to describe the real system, the second task refers to develop LPV) model.

Results shows that the proposed models fit the experimental data with an error lower

than a 3 %. Advanced controllers could be designed using these models. As a first approach a PID controller has been designed. The control objective is leading the controlled variables (temperatures) in order to reach the set point rejecting the disturbances.

Acknowledgements

I would like to express my gratitude to my advisors, Dr. Carlos Ocampo Martínez and Dr. Sebastian Tornil Sin, for their interest, advises and continuous support. They have always been very kind and patient. They gave me the possibility for learning for professional development within the context of applied research.

Thanks to Brais González for offering all his support and knowledge about the pasteurization process. His guidance helped me to understand the physical behaviour. Also I would like to thank Ferran Cortor his help and advises during all the start-up of the small-scale pasteurization plant.

A special gratitude goes to my family for being such a great example of work, courage and perseverance, for their support and motivation. They have always raised me up when I feel falling.

Sandra Terradellas Balaguer

Barcelona, October 2016

Contents

List of Figures

Chapter 1

Introduction

1.1 Motivation

The pasteurization process is one of the most common treatments in milk, fruit juice and beverages industries to sterilise and extend their shelf life. It is based on maintaining a high temperature stablished during a short period of time (HTST). This process is widely used in food industries and it is considered a complex dynamical system with nonlinearities. This strategy avoids undesirable quality changes during the process. This process involves applying heat to the products, during a predetermined period of time and at certain temperature profile in order to eliminate harmful pathogenic and spoilage microorganism.

In the past, the control of pasteurization process was based on maintaining the operation stable and reducing the influence of external perturbations. To accomplish these objectives, a proportional integral derivative (PID) controller was been used with successful results [Cai12]. Although the temperature of the pasteurization process can be controlled with classical control method, changes on the milk temperature are produced

due to disturbances. To minimize the effect of these phenomena, a higher set point temperature was fixed in order to avoid temperatures below the pasteurization one. The result of this increase is a loss of energy caused by a greater heating than it is needed. Further, it can produce alterations in the milks characteristics.

Nowadays, due to the market globalization, the changes in the needs and demands of the costumers and the increasing interest in the environmental problems, the industries have to adopt new advanced control techniques in order to remain competitive and profitable. One of the most used tools is the Model Predictive Control (MPC).

This project deals with the development of a dynamical model for a small-scale pasteurization plant based on physical principles. As nonlinear equations will be obtained, an LPV model based on the first ones will be created. The incorporation of a controller to these models will improve the regulation and track of the temperatures.

1.2 State of art

As mentioned in the previous section, the goal of a pasteurization process is to maintain a high temperature stablished during a short period of time. It consists in different units, generally based on heat exchange, to achieve the product quality desired. Researches on modelling and controlling this type of industrial processes have been strongly supported in the last decades.

To develop a model for a pasteurization process can be very complex considering the different equations involved and time consuming. Meanwhile, empirical model using real data makes the development of a model easier for complex process. Since 1998 different works about pasteurization process can be found in the literature. Ibarrola et al., [JIGS98] presented a model to describe a high temperature short time pasteurization process. Each physical element of the plant was identified separately and the complete process was

considered as a union of single parts. The model proposed was based on real data and it incorporated the nonlinearities from varying flow. Along the same sense, Alastruey et al., [CAGS99] proposed a model for a pasteurization plant based on the structure of [JIGS98]. The main differences from the previous model were that the fundamental physical properties of the plant were not neglected, being the blocks of the heat exchanger of third order. In addition, the delay after the output of the heat exchanger was taken into account.

Using an empirical model, Wan et al., [WWM12] in 2012 determined the best control strategy in pasteurization process of a pink guava puree. The control strategy chosen was the Proportional, Derivative and Integral (PID). In order to improve the control, Khadir [KRRO] proposed a nonlineal model for the plate of the heat exchanger and the usage of Model Predictive Control (MPC) to investigate the benefits over the classical control method (PID).

In 2012, UPC began a new project related to the modelling and control of a pasteurization process using a small-scale plant. Caiza [Cai12] developed a black-box model and designed a predictive control around one working point. Ocampo and Rosich (2015) followed the investigation and implemented some real-time predictive control schemes [ROM15]. In this project a new model is developed for the small-scaler pasteurization plant based on physical principles. Moreover, based on this one, an LPV model is also created. Both models can be used in a wide operation range.

1.3 Objectives

1.3.1 General objective

A pasteurization process is a complex dynamical system with interconnections between their elements. That confers to the system a nonlinear behavior. To control the system, knowledge of the model to predict process behavior is required. Hence, the main goal of the present project is to develop and validate a model for a small-scale pasteurization plant that allows the implementation of advanced real-time control.

1.3.2 Specific objectives

Considering the specific case of the project, the general objective is developed by achieving the following points:

- design a nonlinear model based on physical principles;
- validate the nonlinear model developed using experimental data;
- design a linear LPV model based on the nonlinear model;
- validate the LPV model using experimental data;
- compare the nonlinear to the LPV model;
- design and simulate a PID controllers in order to control the temperatures;

1.4 Overview of the project structure

This project is divided into 6 chapters. Chapter 2 gives a general background of the pasteurization process and presents the different components of the small-scale plant used. Chapter 3 presents how nonlinear model equations are obtained and validated using real data from the system. Chapter 4 formulates an LPV model based on the nonlinear model designed on chapter 3. Chapter 5 gathers the designs of PID controllers and the simulation and analyses of the results obtained with Simulink/Matlab. Finally, chapter 6 gives the main concluding ideas and the further work proposed.

Chapter 2

System description

The plant used in this project is a laboratory version of a real industrial process manufactured by Armfields Process Plants Trainer: the small-scale pasteurization plant PTC23 MKII. It represents an industrial process of high-temperature short-time pasteurization (HTST). The goal of this process is to keep the product at the pasteurization temperature during a minimum period of time stablished.

This system has three main elements: the process unit Figure (2.1),), the control console and the software control. The process unit is connected to the control console in order to monitor on-line the main parameters (temperatures and flows) and control the system. [Arm10]. The product to be pasteurized is fed either in tank A or B (the valve SOL2 allows to choose the tank). The peristaltic pump N1 impulses the product from these tanks to the regeneration phase of the heat exchanger. In this phase, the product is preheated by the effluent of the holding tube. Then, it passes to the heating phase in the same heat exchanger where the product achieves the pasteurization temperature. The product leaves the exchanger at high temperature T4 and flows through the holding tube to maintain the high temperature (pasteurization temperature) during a certain time. At the end of the holding tube, there is a valve (SOL1) that opens in case that

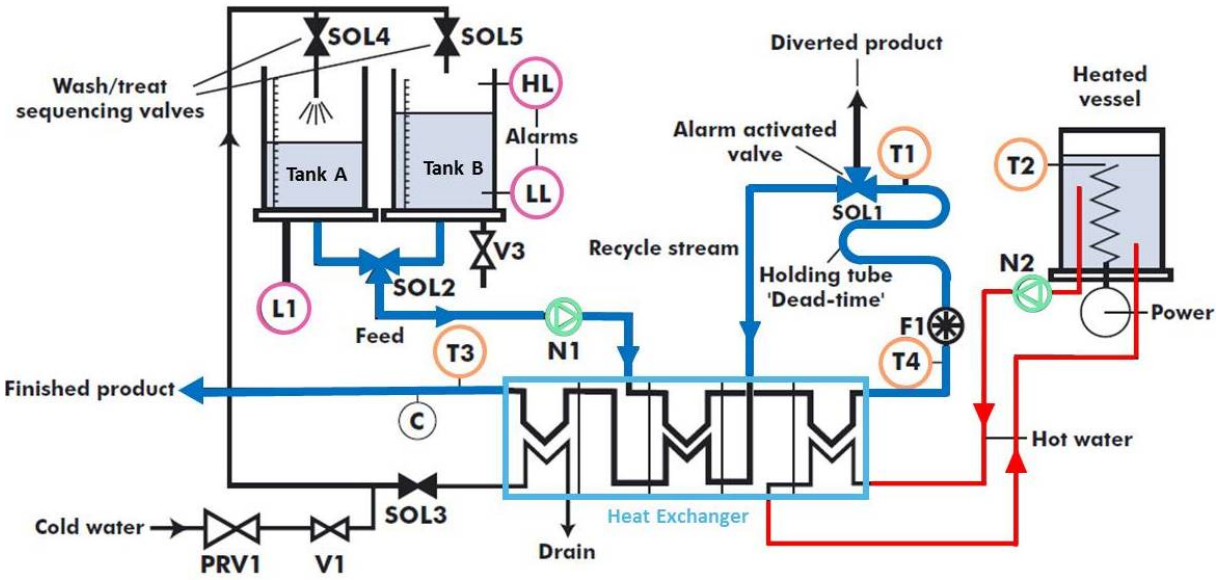

Figure 2.1: Process flow diagram

the temperature at this point T1 is higher than the desired. If the valve is open the fluid returns to the exchanger and passes through two phases. The first one is the regeneration, where its temperature decreases by preheating the product from tank A and B. The second phase is cooling, where the goal is to cool the final product using water as a cooling fluid. On the other hand, when the product temperature is not high enough (T1 is lower than the desired), the valve SOL1 is closed and it sends the product to the feeding tank again.

2.1 Process unit

The process unit refers to the experimental pilot plant (Figure 2.2). The most import elements are:

- Two feeding tanks (Element A of Figure 2.2)
- Heat exchanger (Element B of Figure 2.2)

- Holding tub (Element C of Figure 2.2)
- Hot-water tank (Element D of Figure 2.2)

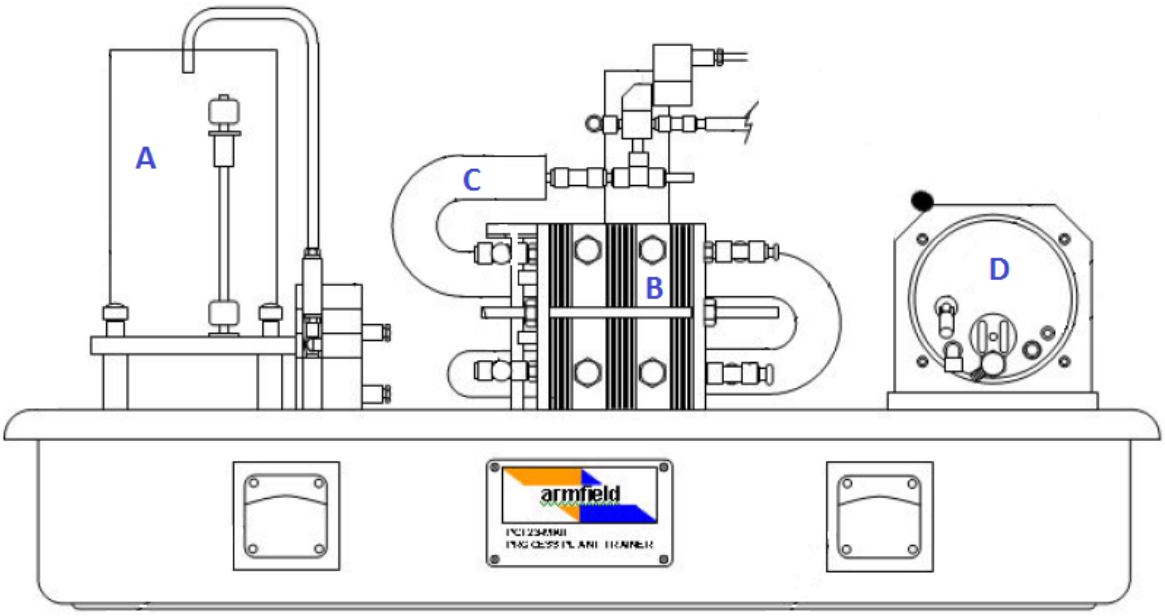

Figure 2.2: Scheme of the process unit

Further, different elements are installed in the pasteurization plant such as valves, pumps and sensors to control and evaluate the system. These elements are presented in the flow diagram of Figure 2.1.

2.1.1 Feeding tanks

The plant PCT23-MKII is provided by two feeding tanks (Figure 2.3) that contain the product to be heated. They are cylindrical glass tanks with volume of 6 l each one. The product is fed in these tanks and the flow is controlled by an electronic valve. A manual valve allows emptying the tank.

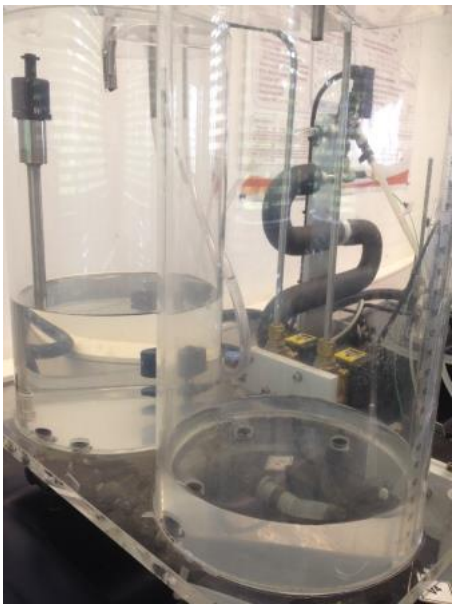

Figure 2.3: Feeding tanks of the experimental plants

2.1.2 Heat exchanger

One of the most important devices of the plant is the heat exchanger. It is a count-current plate exchanger composed of three different phases as can be seen in Figure 2.4. Each plate has an area of 8x11.5 cm^2 and a thickness of 0.18 cm. In the first phase (central part Figure 2.4), called regeneration, the product is pre-heated main by the calorific energy of the end product coming from the holding tube, reducing the energy required in the next phase. The second phase (right part Figure 2.4), named heating, the product reach the pasteurization temperature T4 using hot-water as a heating fluid. Finally, the third phase (left part Figure 2.4) consists of cooling, the end product reduces its temperature before leaving the process with a cold liquid (in this case water). An image of the heat exchanger is presented in Figure 2.5.

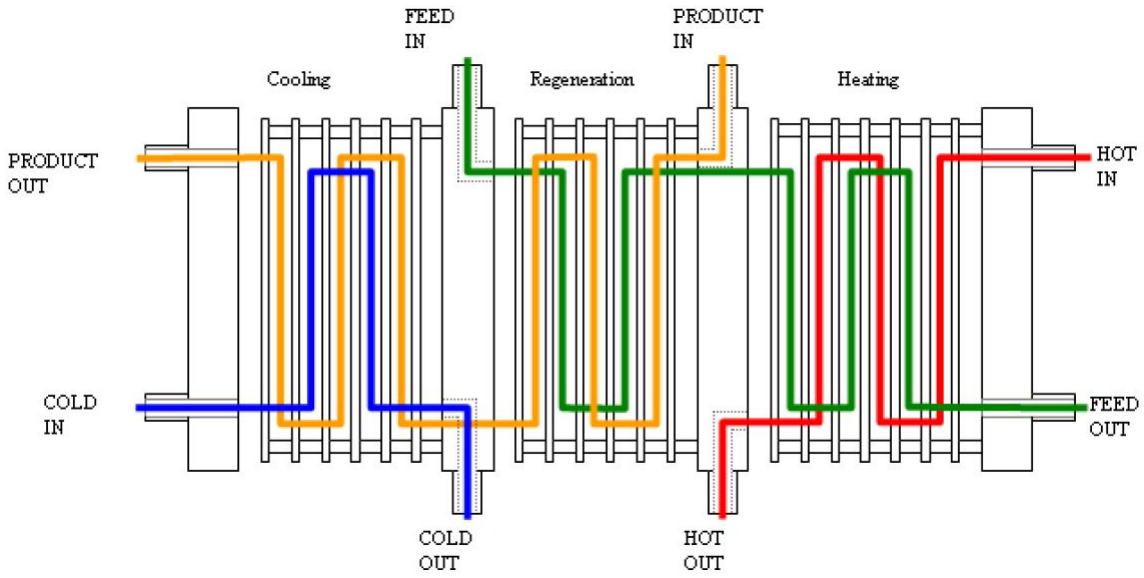

Figure 2.4: Scheme of the heat exchanger

2.1.3 Holding tube

The holding tube (Figure 2.6) is a thermally insulated tube with a length of 60 cm and an internal diameter of 13.2 cm. It allows maintaining the temperature of the product by a certain time, being this time controlled by the flow. If at the output of the tube the temperature is still higher than a specific value, the pasteurization will be achieved.

2.1.4 Hot-water tank

Water is the hot fluid used in the heat exchanger on the heating phase (Figure 2.4). It is heated in a cylindrical tank (Figure 2.7) with a radio of 7.5 cm and a length of 20.5 cm, by means of an electrical resistor (power of 0-2.5 kW). Depending on the power and the efficiency of the heat exchanger, the flow can be modified by changing the speed of the hot-water pump, N_2. The temperature inside the tank T_2 is controlled by the power of the resistor and the speed N_2.

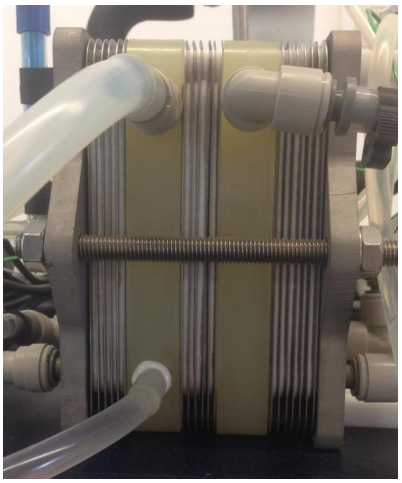

Figure 2.5: Heat exchanger of the experimental plant

2.1.5 Valves

The plant has five solenoid operated valves that can be controlled by the control console or the PC. They are represented in the flow diagram of Figure 2.1 and can be described as follow:

- SOL1: Product-divert solenoid valve
- SOL2: Feeding-select solenoid valve, tank A or tank B
- SOL3: Product-cooling solenoid valve
- SOL4: Tank-A-fill solenoid valve
- SOL5: Tank-B-fill solenoid valve
- PRV1: Pressure-reducing valve
- V1: Flow-control valve

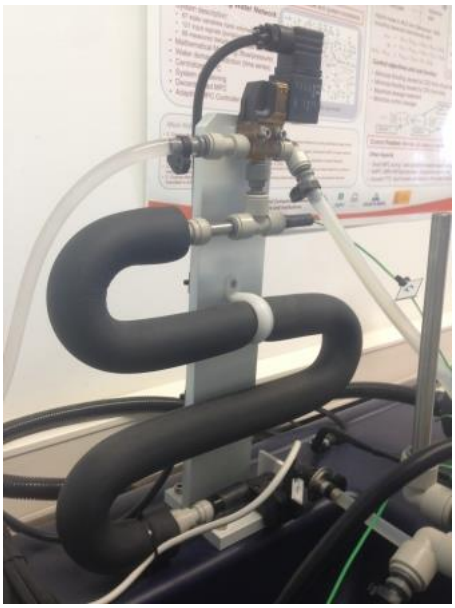

Figure 2.6: Holding tube of the experimental plant

2.1.6 Pumps

The process unit also incorporates two peristaltic pumps (Figure 2.8). One impulses the product from the tanks feed tanks A and B to the heat exchanger (Figure 2.1). The other one pumps the hot-water from its tank to the heat exchanger (Figure 2.1). Their speeds belong to the range [0, 400] rpm. These peristatic pumps of the plant are named as follow:

- N1: Feeding pump
- N2: Hot-water pump

2.1.7 Sensors

Different sensors are installed in the pilot plant to monitor in certain points the temperature, level of tanks and flow.

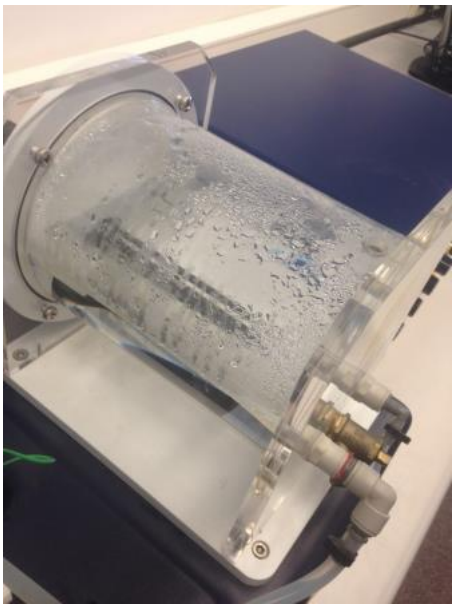

Figure 2.7: Hot water tank of the experimental plant

Temperature sensor: There are four temperature sensors that monitor the temperature at four important points (Figure 2.1). These sensors give a measure between 0 and 150°C of the following key points:

- T1: Holding tube exit
- T2: Hot-water temperature
- T3: Outflow temperature
- T4: Heated product temperature

Tanks A and B are equipped with a level sensor. Tank A level sensor L_1 gives a direct measurement of the product level at tank A in the range [0, 250] mm. In contrast, the tank B has two fixed float switches (LL and HL) as level sensors. The first one detects the low level and the other detects the high level.

Figure 2.8: Hot-water pump implemented in the experimental plant

A turbine-type flow sensor F_1 is installed at the entrance of the holding tube to measure the product flow rate. The measured range is between 0 and 500 ml/min.

2.2 Control console

The control console allows the user to monitor and control the plant either manually or by the PC. The principal elements of the panel can be seen in Figure 2.9. There are three groups of potentiometers plus on/off switches that permit to regulate the speed of the hot-water pump N_2, the feeding pump N_1 and the power of the electric resistor P (1-2-3 in Figure 2.9) manually. The selectors (4-5-6 in Figure 2.9) allow choosing the operation mode that can be manually, USB or with voltage externally supplied. Further, the measurement chosen with the selector number 7 can be displayed on the screen. Finally, the selector number 9 decides between either manually or USB operation of the solenoids valves (10, 11, 12, 13 and 14 in Figure 2.9). An image of the control console is

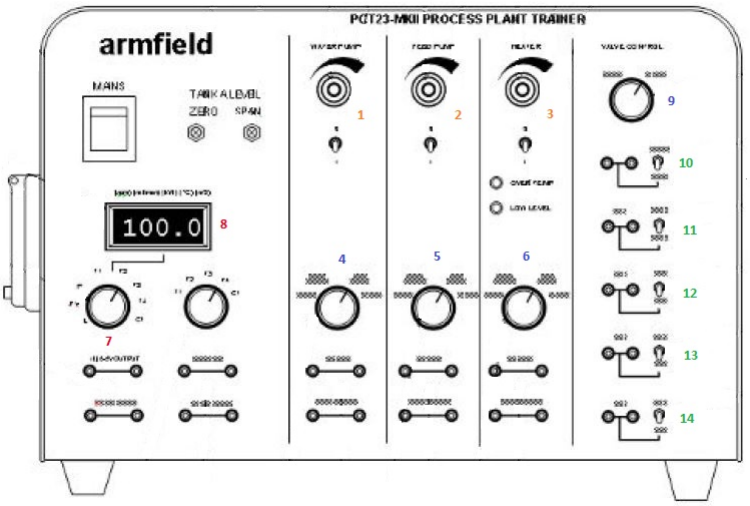

Figure 2.9: Scheme of the control console implemented in the experimental plant

presented in Figure 2.10.

2.3 Software control

The software control, allows the communication between the control console and the PC by using an USB cable. Executing the program ArmSoft PCT23 Process Plant Trainer (Figure 2.11) the monitoring of the pilot plant in real-time start. The software registers the data and allows implementing different PID strategies to regulate the temperatures.

Figure 2.10: Control console image

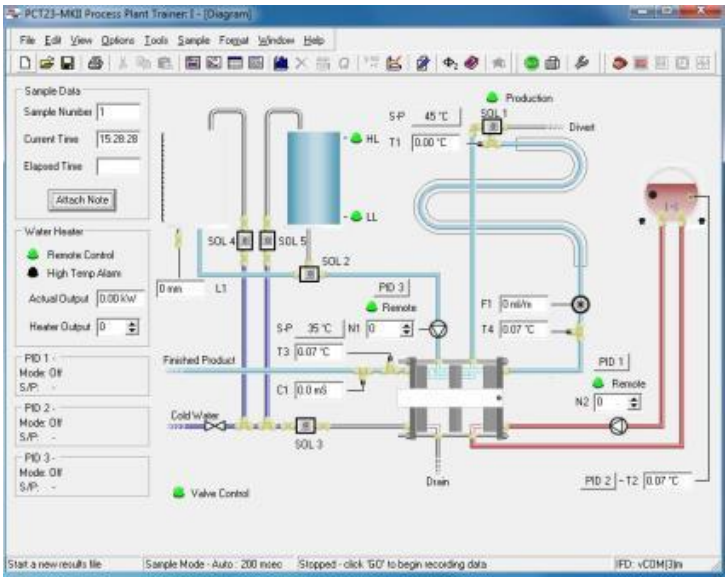

Figure 2.11: Program ArmSoft PCT23 Process Plant Trainer interface

Chapter 3

Nonlinear modelling and experimental validation

Models allow expressing relations between different variables and parameters of a system in order to study its behaviour.

The knowledge of the dynamical response of each one of the elements of the pasteurization plant is fundamental in order to control it. Therefore a fundamental objective of this Master project is to develop a dynamical model for the PTC23-MKII plant. There are two ways to develop a model [Lju87]; one is using the physical principles that describe the system (theoretically) and the other one is using the system identification from experimental data (experimentally). Due to the number of variables of the system and taking into account that the system can be described by physical process, a parametric model has been proposed. It is characterized by a finite set of parameters.

To develop the model, the plant has been divided in 5 elements to be modelled: feeding pump, hot-water pump, hot-water tank, holding tube and heat exchanger. Physical principles based on fundamental laws such as energy balances and heat exchanger design

are used to describe the main processes of the plant [HR04] [JCLA94]. Figure 3.1 shows a schema of all the elements, its variables and their nomenclature.

In this chapter, the model for each element is presented. Further, the constant parameters are determined by experimental data and finally the models are validated.[1]

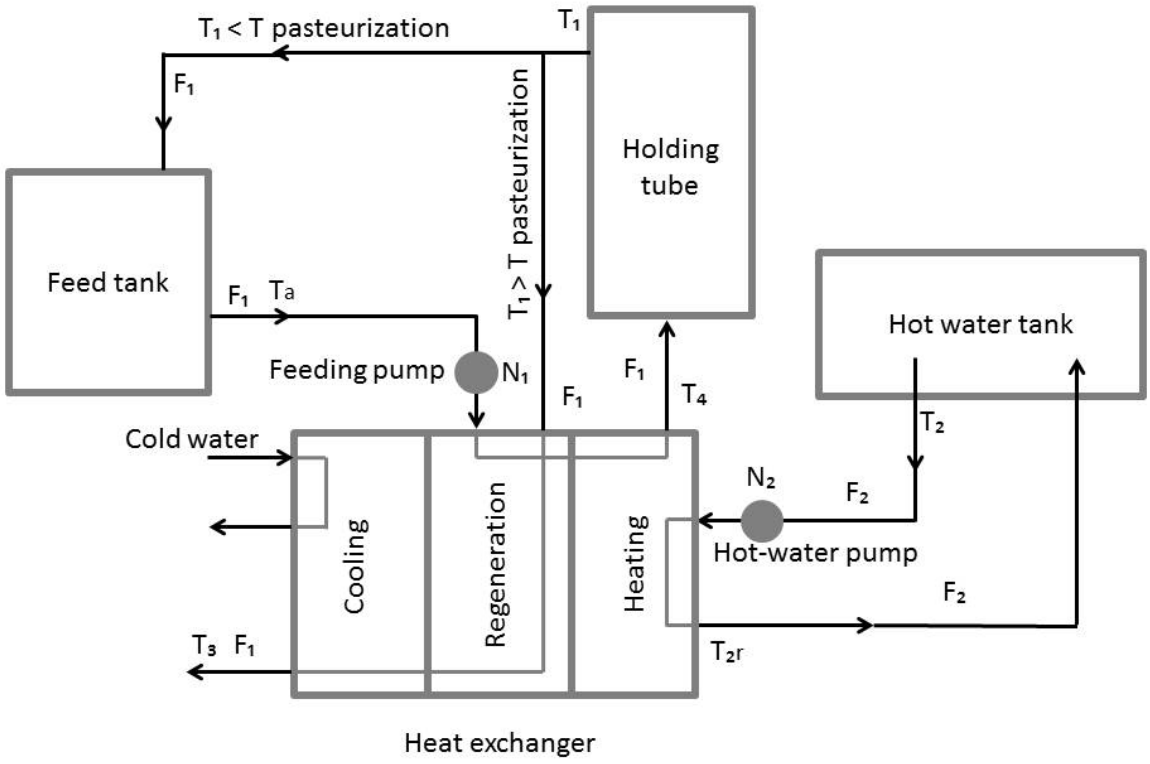

Figure 3.1: Scheme of the six subsystems and their connections

[1]The temperatures, flows, power and speeds presented in the document are time-dependent. To reduce the complexity of the notation, the time-dependent notation (t) has been omitted

3.1 Feeding pump model

A peristaltic pump is a positive displacement pump based on alternating compression and relaxation. The fluid flows through a flexible tube fitted inside a circular casing. The rotor with two rollers is attached to the case comprising the tube. While the rotor is turning, the part of the tube with compression closes, forcing the fluid to be pumped and moved to the lowest output [WM].

The feeding pump (labelled by its speed, N_1) is the one that impulses the product to be treated from the feeding tank to the heat exchanger (Figure 3.1). The pump model correlates the speed of the pump N_1 with the fluid flow through the tube F_1. This model is based on experimental data extracted from a flow meter installed in the plant. Figure 3.2 presents the flow rate F_1 for different values of rotor speed N_1, in percentage. The blue line represents the experimental flow increasing the pump speed in steps of 5 % and the green line the experimental flow decreasing 5 % the pump speed. Finally, the red line represents the fitting curve. The graphic shows a linear correlation for speeds higher than 20 % described by the following equation:

$$\begin{aligned} F_1 &= 4.1170N_1 - 81.9020, \\ &= k_{N1}(N_1 - 20), \\ &= 4.1120(N_1 - 20), \\ &= 0.0685(N_1 - 20). \end{aligned} \tag{3.1}$$

By 3.1 the value of the gain in static state of the pump can be computed. It can be considered that the change of the speed immediately produces a change of flow. Further, the flow (in ml/s) obtained in 3.1 is the same of the mass flow expressed in g/min taking into account the density (water).

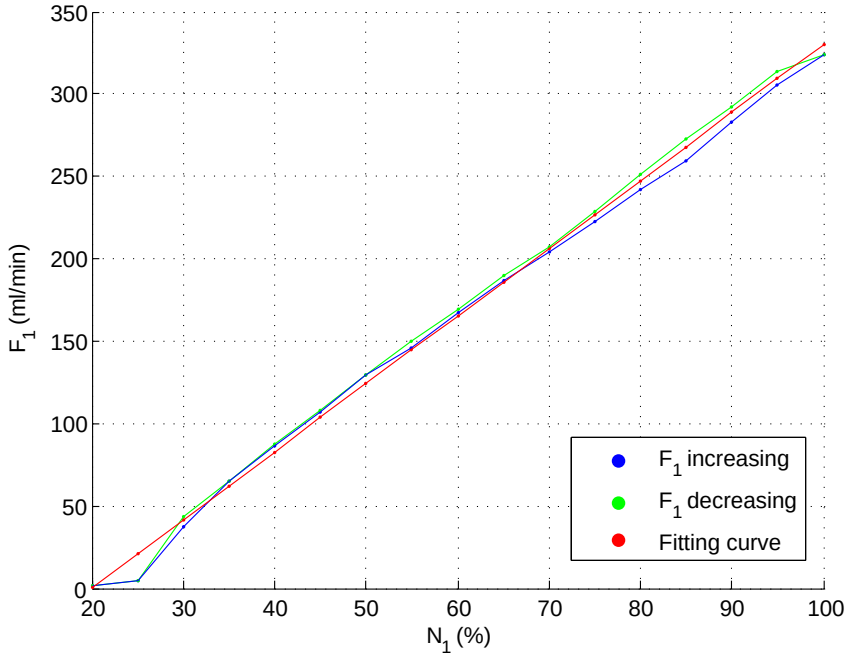

Figure 3.2: Experimental relationship between the flow rate F_1 and rotor speed of the feeding pump N_1

3.2 Hot-water pump model

The hot-water pump impulses the hot-water from the hot-water tank to the heat exchanger (Figure 3.1). The same procedure as pump N_1 has been followed to determine the correlation between speed of the pump N_2 and the flow F_2. However, in this case, a flow meter is not installed therefore the flow has been experimentally determined at each speed.

By measuring the volume collected during a period of time. The output tube from the hot-water tank has been connected to the feeding tank A measuring the volume with the level sensor. During the experiments the speed N_2 has been increased and decreased in steps of 5 %.

Figure 3.3 shows the flow rate F_2 for different values of rotor speed N_2, in percentage. The blue line represents the experimental flow increasing the pump speed in steps of 5 % and the green line the experimental flow decreasing a 5 % the pump speed. Finally, the red line represents the fitting curve The equation in range 20 % (that is when the water

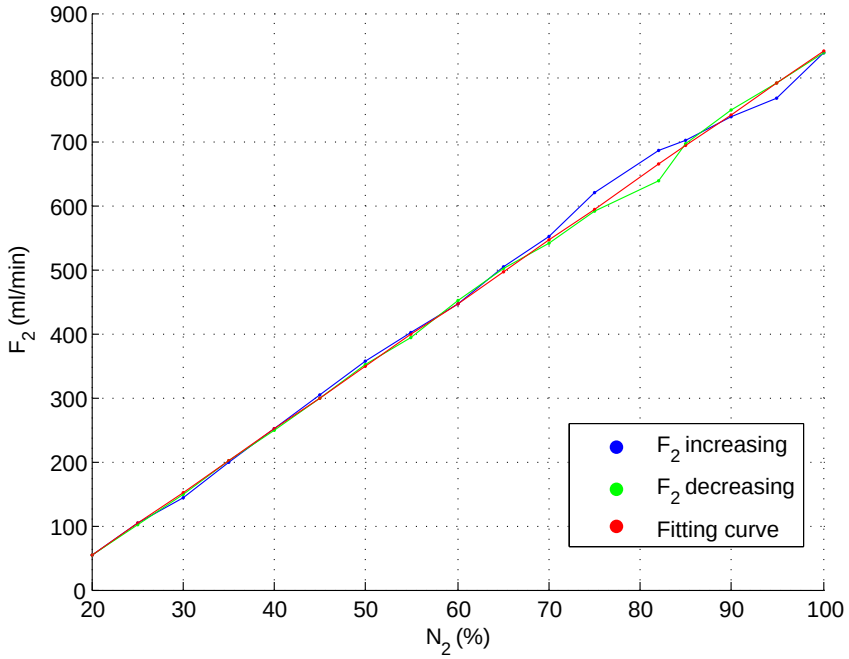

Figure 3.3: Experimental relationship between the flow rate F_2 and speed of the hot-water pump N_2

starts to flow) to 100 % of speed is described as:

$$\begin{aligned} F_2 &= 9.8223N_2 - 142.1700, \\ &= k_{N2}(N_2 - 20), \\ &= 11.1187(N_2 - 20), \\ &= 0.1853(N_2 - 20). \end{aligned} \tag{3.2}$$

As with the feeding pump, it can be considered that the change of the speed immediately produced the change of flow. The flow obtained in this equation (in ml/s) is the same of

the mass flow expressed in g/min taking into account the density (water).

3.3 Hot-water tank model

The hot-water tank maintains the water at high temperature T_2. This thermal energy is used in the heat exchanger to the pasteurization process. Hot-water leaves the tank at a temperature T_2 and goes to the heat exchanger. When the exchange is done, it returns to the tank at a lower temperature T_{2r}. The value of this temperature depends on the speed of the hot-water pump N_2.

Three different heat transfer processes may be considered in this system as schematized in 3.4:

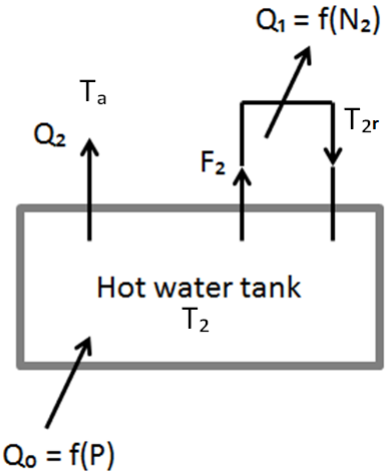

Figure 3.4: Scheme of the hot water tank

- The heated system of the tank based on a resistance sunk in the water tank. The heat transferred (Q_0) depends on the power resistor applied P. The power is ranged from 0 W up to 1600 W.

- The loss of heat due to the recirculation flow in the heat exchanger (Q_1), expressed by the following equation:

$$Q_1 = F_2 C_a (T_2 - T_{2r}), \tag{3.3}$$

  where C_a (J/K) is the specific heat of the water and F_2 is the mass flow of hot-water that flows to the heat exchanger and returns. T_2 is the temperature inside the reactor and T_{2r} is the returned water temperature from the heat exchanger.

- The heat loss to the environment (Q_2) described by the convection equation [JS07]:

$$Q_2 = UA(T_2 - T_a), \tag{3.4}$$

  where U ($\mathrm{Wm^2/K}$) is the constant of convective heat transfer, A ($\mathrm{m^2}$) is the area of the tank and T_a (°C) is the room temperature.

Applying an energy balance to the hot-water tank system, the equation can be defined as:

$$\begin{aligned} C_i \frac{\mathrm{d}T_i(t)}{\mathrm{d}t} &= \sum_{ij} E_{ij}(t), \\ C_A \frac{\mathrm{d}T_2(t)}{\mathrm{d}t} &= P - F_2 C_a (T_2 - T_{2r}) - UA(T_2 - T_a), \\ &= P - k_{N2}(N_2 - 20) C_a (T_2 - T_{2r}) - UA(T_2 - T_a), \\ &= P - k_1 (N_2 - 20)(T_2 - T_{2r}) - k_2 (T_2 - T_a), \end{aligned} \tag{3.5}$$

where C_A (J/K) is the calorific capacity of the water of the hot-water tank, $k_1 = k_{N2} C_a$ and $k_2 = \mathrm{UA}$.

The differential equation 3.5 is nonlinear as it has the product of two variables N_2 and T_2. The actuators of this element are the power of the electrical resistor P and speed of the hot-water pump N_2. Further, 3.5 considers three temperatures T_2, T_{2r} (output and input of the hot-water tank) and Ta (room temperature) that are measurable variables. Finally, the constant parameters k_1 and k_2 are determined by adjusting experimental data and the parameter C_A by considering the characteristics and proprieties of the system

3.3.1 Calorific capacity of the water of the hot-water tank (C_A)

The calorific capacity C_A (J/°C) is the product of the specific heat (Cp) of the hot-water and the mass M in (g) that there is in the hot-water tank, i.e,

$$C_A = C_p M. \tag{3.6}$$

The value of the specific heat is 4.18 J/g°C considering pure water at constant temperature [Wea88]. To calculate the mass of liquid inside the tank , the internal volume of the tank and the density of the liquid ($1000 kg/m_3$) are taken into account. Notice that the hot-water only takes up half of the volume of the tank. Starting from equation 3.6, the new expression of the calorific capacity takes the following form:

$$\begin{aligned} C_A &= C_p \rho \mathrm{V}, \\ &= C_p \rho \pi \mathrm{r}^2 L_{\overline{2,}} \end{aligned} \tag{3.7}$$

where r is the radius in cm of the hot water tank and L is the length also in cm. Substituting, the final value is 7524 J/°C

3.3.2 Parameter $\mathbf{k_2}$

To experimentally determine this constant, the recirculation flow has been closed. At these conditions Q_1 is null (Figure 3.4). Then, the equation 3.5 can be rewritten as

$$C_A \frac{\mathrm{d}T_2(t)}{\mathrm{d}t} = P - k_2(T_2 - T_a). \tag{3.8}$$

The power value has been fixed at a 2 % (50 W) and the room has been measured

being 24.4 °C. Taking into account these values, the equation 3.8 can be expressed as:

$$\begin{aligned} \int_0^t \mathrm{d}t &= 7524 \int_{T_0}^{T_2} \frac{1}{P - k_2(T_2 - T_a)} \mathrm{d}T_2, \\ t &= \frac{1}{-k_2} \ln(P - k_2(T_2 - T_a))\Big|_{T_0}^{T_2}, \\ &= \frac{7524}{-k_2} \ln\left(\frac{P - k_2(T_2 - T_a)}{P - k_2(T_0 - T_a)}\right), \end{aligned} \tag{3.9}$$

where t represents time in seconds.

To find the value of the parameter k_2 a trial and error method has been used to adjust the experimental data to 3.9. Experimental data T_2 vs t is represented in a red curve in Figure 3.5. Different values of k_2 have been tested in order to see which one fits better to the real data. In Figure 3.5 the different curves are compared. The blue curve represents k_2 = 1.20 J/s°C, the green curve k_2 = 1.25 J/s°C and the light blue curve k_2 = 1.30 J/s°C. The blue curve is the one that follows better the real data when is reaching the steady state. This value is considered in the model of the component hot-water tank 3.5.

3.3.3 Parameter $\mathbf{k_1}$

To determinate the constant parameter k_1, another experiment has been designed. The actuators have been fixed to a constant value, N_1 and N_2 at 40 % and P at 205 W to reach the steady state. At that point, the variation of T_2 is null and the difference between T_2 and T_{2r} is constant. Then, the system expressed in 3.5 can be described by the following equation:

$$0 = P - k_1(N_2 - 20)(T_2 - T_{2r}) - k_2(T_2 - T_a). \tag{3.10}$$

Figure 3.6 shows the evolution of experimental temperatures T_2 (blue curve) and T_{2r} (red curve) until they reach the steady state being the values of T_2 and T_{2r} at this point

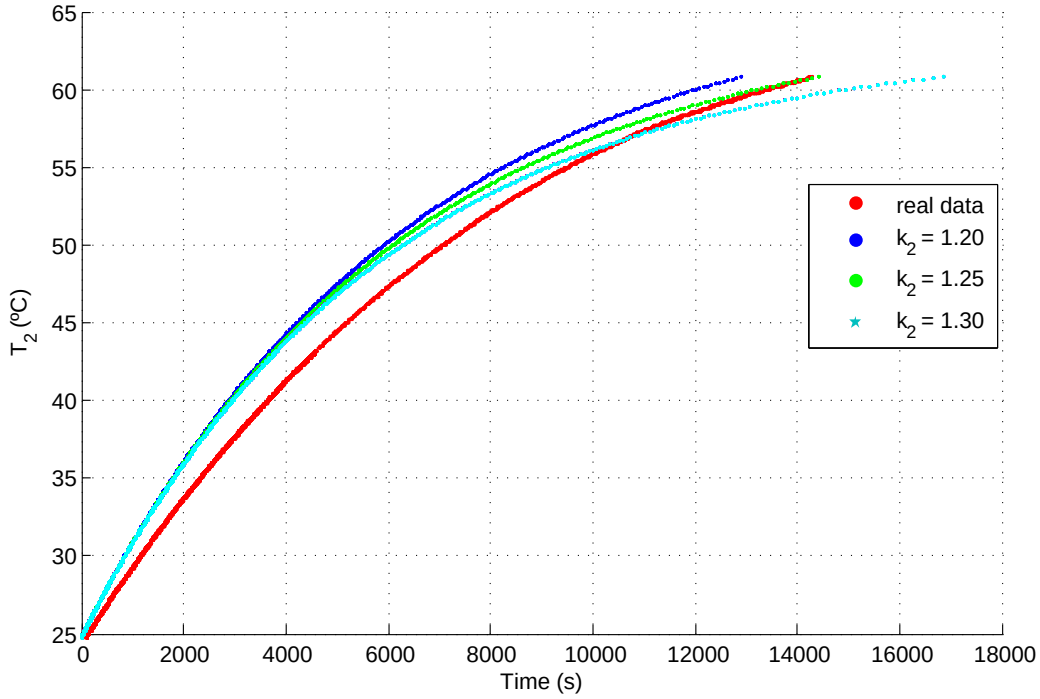

Figure 3.5: Variation of T_2 for different values of the constant k_2

are 68.5 °C and 46.5 °C, respectively and the room temperature 23.5 °C. Considering this values and equation 3.10, k_1 can be calculated and has a final value of 0.4 J/s°C. Taking into account all the parameters calculated in this section, the final equation proposed for the hot-water tank can be expressed as:

$$7524\frac{\mathrm{d}T_2(t)}{\mathrm{d}t} = P - 0.4(N_2 - 20)(T_2 - T_{2r}) - 1.20(T_2 - T_a). \tag{3.11}$$

3.4 Holding tube

The holding tube is a tube covered with an insulation material. The main finality of this tube is to maintain the high temperature (pasteurization temperature) during a period of time. The influent comes from the first stage of the heating exchanger (heating phase, Figure 3.7) at a flow rate F_1 and high temperature T_4. The input temperature

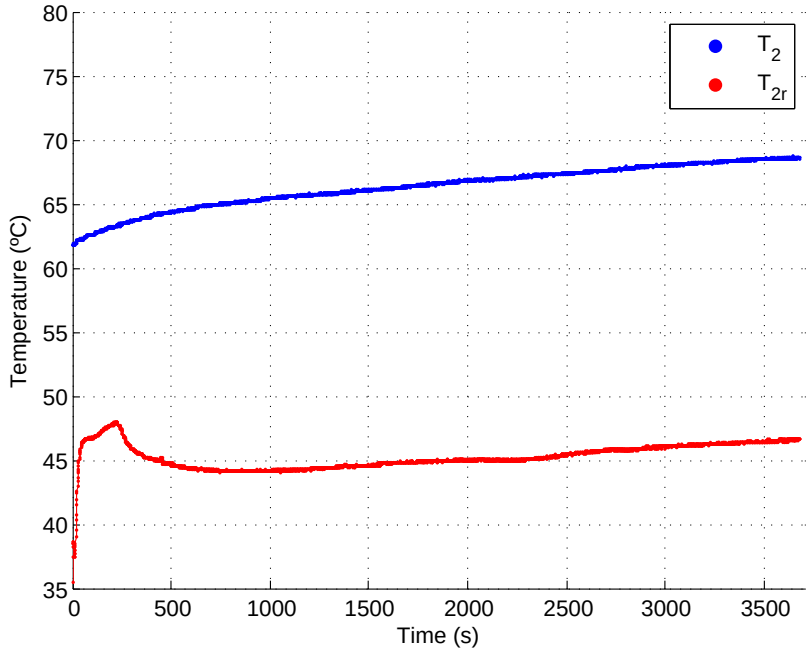

Figure 3.6: Evolution of the temperatures T_2 and T_{2r}

has been considered the same that at the output of the heat exchanger T_4 as there is not a sensor installed at this point. This assumption is based on the proximity of these two points.

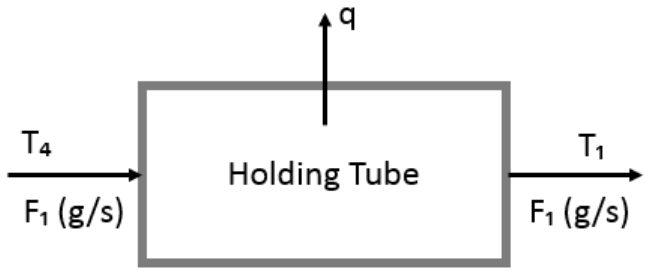

Figure 3.7: Scheme of the holding tube

Although the tube is isolated, head loss is expected. Small flow heat (Figure 3.7) is transferred to the environment producing a decrease of the effluent temperature. Also,

a delay should be considered depending on the flow rate of the product [GGI01]. This delay in seconds can be calculated with the following equation:

$$\begin{aligned} \tau &= \frac{\text{Volume}}{F_1}, \\ &= \frac{82}{F_1}. \end{aligned} \tag{3.12}$$

An experiment has been performed in order to test the precision of 3.12. It consists in changing suddenly the temperature T_4 and determine the effect over T_1. To change the temperature T_4 the speed of the feeding pump N_1 has been decreased from 60 % to 40 %. With these conditions T4 increases because there is less total volume of product to heat.

The theoretical value of the delay τ, obtained with (3.12) and a product flow of 94 ml/min, is 52 s. Figure 3.8 shows the result of the experiment where the value of τ is 51 s, being the relative error 1.92 %. Assuming a mean temperature T_{int} inside the holding

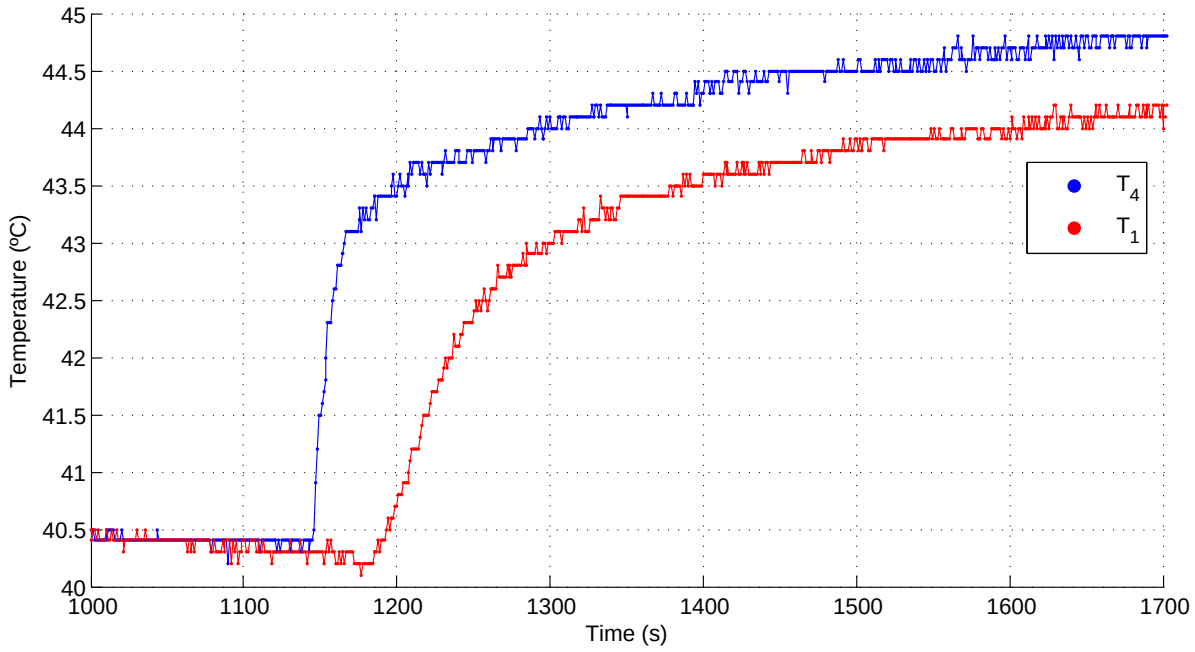

Figure 3.8: Evolution of the temperature T_4 and T_1

tube, the energy balance can be described by:

$$Q = F_1 C_p \Delta T + M_1 C_p \frac{\mathrm{d}T_{int1}}{\mathrm{d}t}, \tag{3.13}$$

where Δ T=T_1(t)-T_4(t-τ) is the variation of temperature between the output (T_1) at the instant t and the input (T_4) at the instant $t-\tau$ s and $\frac{\mathrm{d}T_{int1}}{\mathrm{d}t}$ is the variation of the internal mean temperature in the tube ($T_{int1} = \frac{T_1+T_4}{2}$). To calculate the mass of liquid M_1, the internal volume of the tube (82 cm^3) and the density of the liquid (1000 kg/m^3) are considered, i.e. 82 g.

To describe the heat lost in the system Q, the general design equation for head exchanged is considered [HR12]. Due to not have the characteristics and measures of the isolation material a generic coefficient of heat transfer U has been considered:

$$\begin{aligned} Q &= -AU\Delta T_{ml}, \\ &= -AU\frac{(\Delta T_1) - (\Delta T_4)}{ln\left(\frac{\Delta T_1}{\Delta T_4}\right)}, \\ &= -AU\frac{(T_1 - T_a) - (T_4 - T_a)}{ln\left(\frac{T_1 - T_a}{T_4 - T_a}\right)}, \end{aligned} \tag{3.14}$$

where U is the global head transfer coefficient, A is the internal area in contact with the isolated material that has a value of 0.0248 m^2. Moreover, ΔT_{ml} is the logarithmic mean temperature. As the mean temperature T_{int1} has been considered inside the whole tube, the equation 3.14 changes into:

$$\begin{aligned} Q &= -AU\Delta T, \\ &= -AU(T_{int1} - T_a), \\ &= -AU\left(\frac{T_1(t) + T_4(t-\tau)}{2} - T_a\right). \end{aligned} \tag{3.15}$$

The U value has been determined by experimental data. During the experiment different hot-water pump speeds has been tested in order to evaluate if it influences over

U. The other actuators N_1 and P have been fixed to a constant value 50 % and 175 W, respectively.

Results have demonstrated that the value of U is positive and remain constant at different pump speeds (Figure 3.9). Concretely it is 10 W/K m^2 . The final equation of

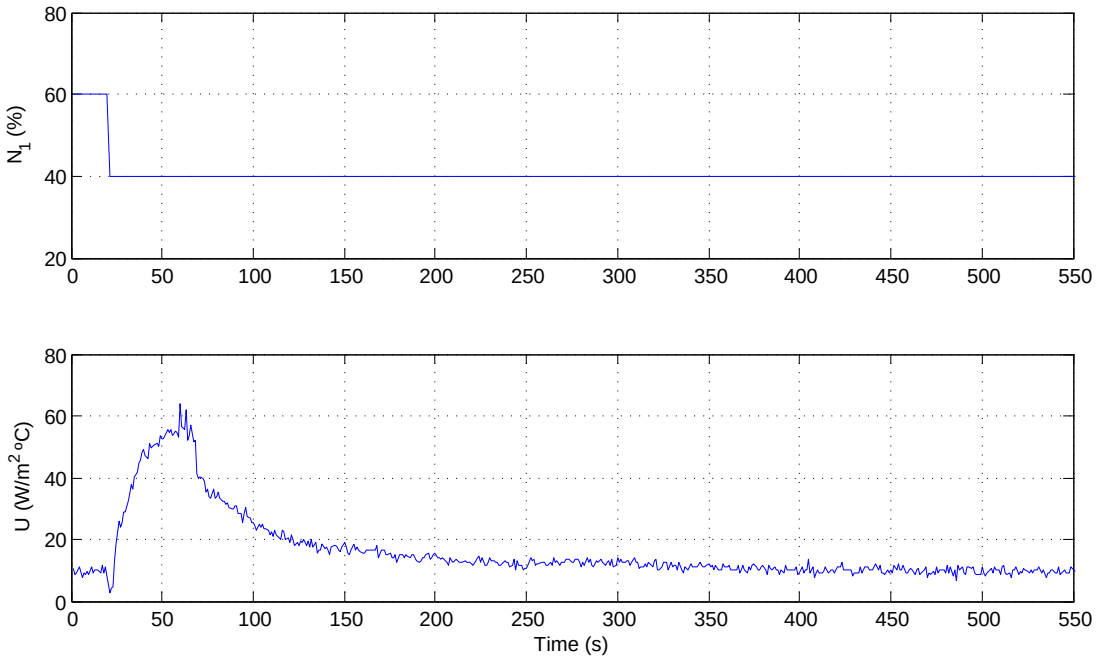

Figure 3.9: Research of the parameter U

the holding tube taking into account the delay and the equations 3.13 and 3.15 can be expressed as:

$$F_1 C_p (T_1(t) - T_4(t-\tau)) + M_1 C_p \frac{\mathrm{d}T_{int1}}{\mathrm{d}t} = -UA\,(T_{int1} - T_a)\,. \quad (3.16)$$

3.5 Heat exchanger

The heat exchanger is the device that allows the thermal energy exchange without mixing the liquids. Heat exchange is controlled by the influent temperature of the fluids

and their mass flow. The heat exchanger of this project had three phases each one with a different finality: heating, regeneration and cooling (Figure 3.10).

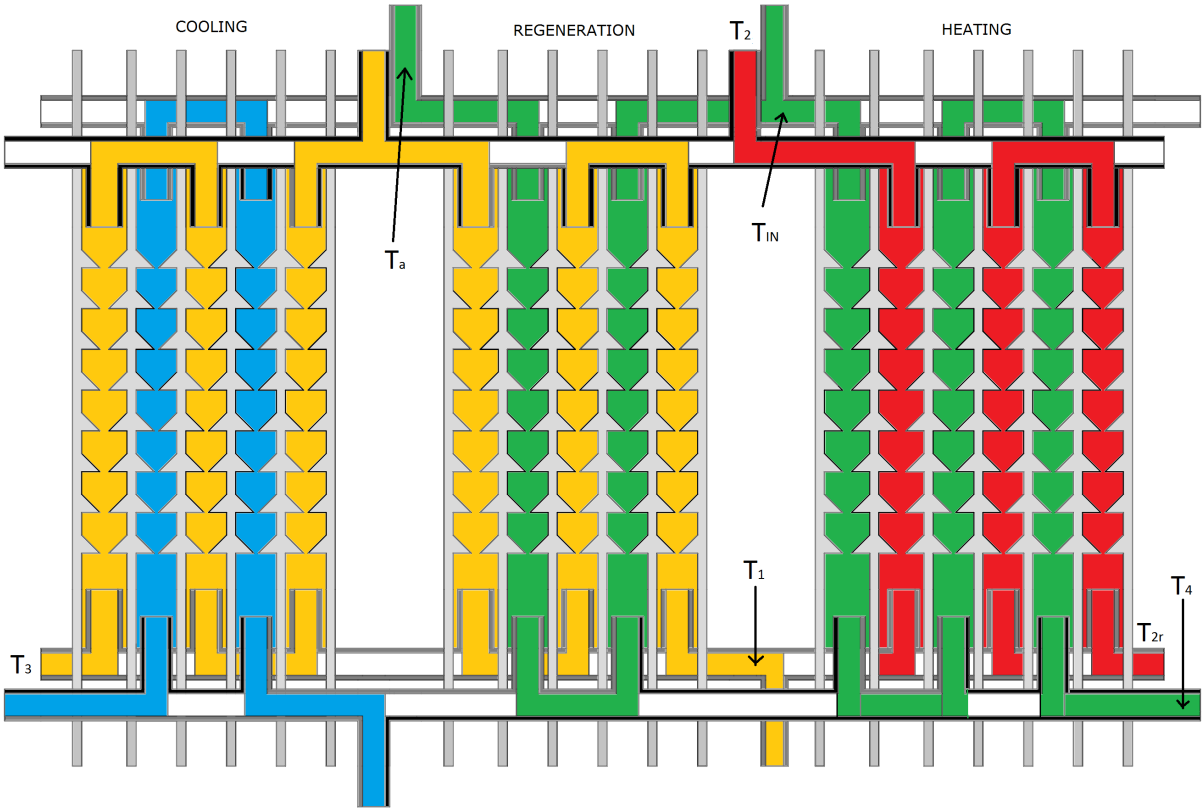

Figure 3.10: Scheme of the different temperatures and flows of the heat exchanger

The first phase, named heating, permitted to head the product from the influent temperature (T_{in}) to the pasteurization temperature. The second phase, regeneration; recuperates calorific energy from end product to reduce the energy required in the first phase. Finally, the third phase, called cooling, the temperature of the pasteurized product is reduced before leaving the system by means of a cold liquid (in this case water).

As mentioned before, the goal of the present project is to control the temperature T_1, hence, only heating and regeneration phases have been considered. Furthermore, each phase operates at different conditions therefore, a model of each phase is developed.

3.5.1 Heating phase

To propose a model of the heating phase, an experimental assay has been performed focused on this stage. With this objective, the regeneration phase has been stopped (closing the valve SOL1) therefore, the effluent of the feeding tank is the influent of the heating phase at the same temperature ($T_{in} = T_a$, see Figures 3.1 and 3.11).

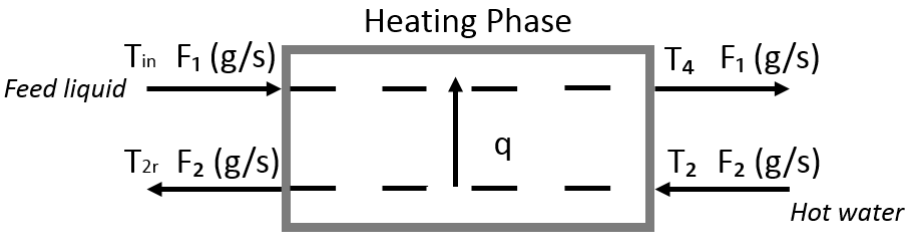

Figure 3.11: Scheme of the heating phase process

On the other side, there is not a temperature sensor in the output of the exchanger. To monitor T_{2r} (water temperature that returns to the hot-water tank), the sensor of the product temperature (T_3) has been moved to that point.

To express the model of the heating phase, an energy balance in dynamic conditions is proposed:

$$\begin{aligned} \text{Feeding} - \text{product} : q &= \dot{m} C_p \Delta T_{feed} + M_2 C_p \frac{\mathrm{d}T_{int2}}{\mathrm{d}t}, \\ \text{Hot} - \text{water} : q &= \dot{m} C_p \Delta T_{HWT}, \\ F_1 C_p \Delta T_{feed} + M_2 C_p \frac{\mathrm{d}T_{int2}}{\mathrm{d}t} &+ Q_{loss1} = F_2 C_p \Delta T_{HWT}. \end{aligned} \tag{3.17}$$

where $\dot{m}$ is the mass flow (F_1 corresponding to the feed product and F_2 to the hot-water) in g/s, $\Delta T_{feed} = T_4 - T_{in}$ is the variation of product temperature between output T_4 and input T_{in} being T_in in this experiment the temperature in the feeding tank T_a. In addition, M_2 is the product mass inside the exchanger and $\frac{\mathrm{d}T_{int2}}{\mathrm{d}}$ is the variation of the internal mean temperature of the product in the heating phase $\left(T_{int2} = \frac{T_4 + T_{in}}{2}\right)$. Finally,

$\Delta T_{HWT} = T_2 - T_{2r}$, where T_2 is the temperature inside the hot-water tank and T_{2r} the temperature of the water when it returns to the hot-water tank.

To calculate the product mass M_2, the internal volume of the heating phase (V, with a value 73.6 cm^3) and the density of the product (in this case water, 1000 g/l) has been considered, i.e, 73.6 g.

The heat exchanger is not isolated therefore a heat loss to the environment Q_{loss1} should be considered. Figure 3.12 shows the influence of the speed of feeding pump (N_1) and water temperature inside the hot-water tank T_2 over the heat loss in the heating phase of the exchanger. Taking into account the results presented in Figure 3.12, a model

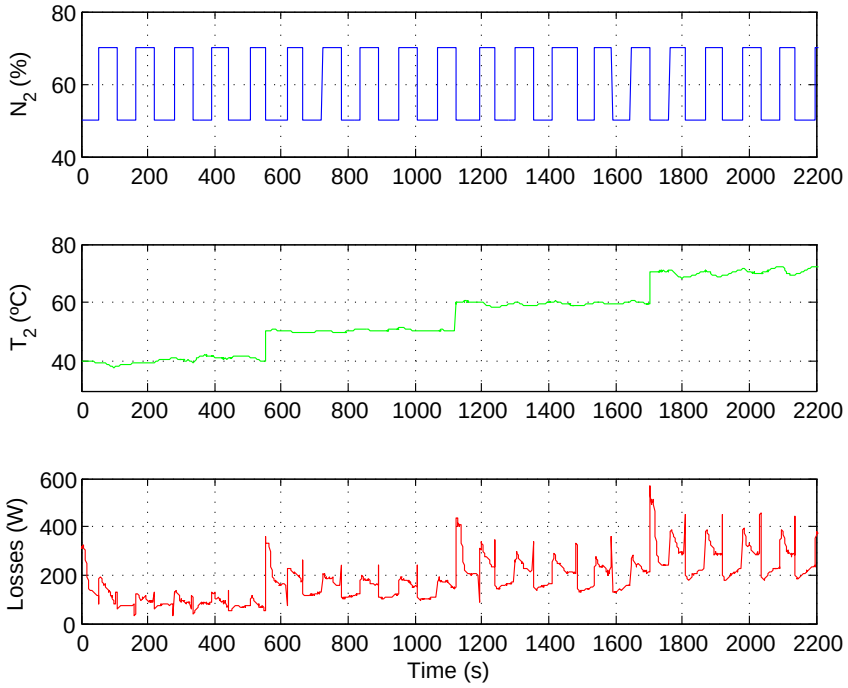

Figure 3.12: Evolution of the feeding pump speed (N_1), the effluent temperature (T_2) of hot water and heat losses on the heating phase of the exchanger

is proposed to determinate the Q_{loss1} considering the periods of stable temperature. This

equation can be expressed as a function of T_2 and N_1:

$$Q_{loss1} = (0.1350N_1 - 0.4990)(T_2 - 27)[\mathrm{W}]. \tag{3.18}$$

Figure (Figure 3.13) correspond to the validation of the losses equation 3.18. The blue curve represents the losses obtained from real data and the red curve the losses using 3.18. Starting from 3.13, the new equation for the heating phase taking into account equation

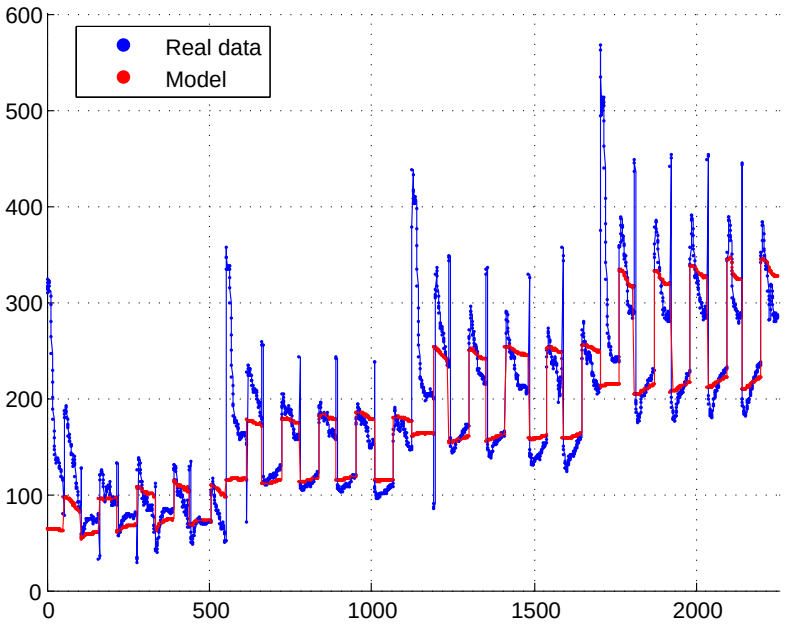

Figure 3.13: Comparison of the real losses (blue curve) with the losses calculated with 3.18 (red curve)

3.18 can be expressed as:

$$F_1 C_p \Delta T_{feed} + M_2 C_p \frac{\mathrm{d}T_{int2}}{\mathrm{d}t} + (0.1350N_1 - 0.4990)(T_2 - 27) = F_2 C_p \Delta T_{HWT}. \tag{3.19}$$

3.5.2 Regeneration phase

In the regeneration phase, the product from the feeding tank at a temperature T_a is preheated to reach T_{in} using as liquid heater the final pasteurized product (Figure 3.14). With this configuration, part of the energy used in the pasteurization process in reused in the own system. To extract experimental data of this phase, the heating phase of the heat exchanger has been stopped. The water of the hot-water tank has been used as the

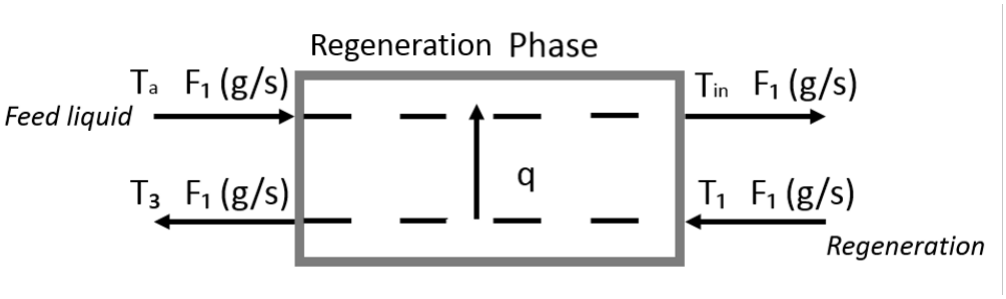

Figure 3.14: Scheme of the regeneration phase process

pasteurized product in order to have a defined value of T_1. This temperature has been controlled with the power resistor P installed in this tank,

To express the model of the regeneration phase, an energy balance in dynamic conditions is proposed:

$$\begin{aligned} \text{Feeding} - \text{product} : q &= \dot{m} C_p \Delta T_{feed} + M_3 C_p \frac{\mathrm{d}T_{int3}}{\mathrm{d}t}, \\ \text{Pasteurized} - \text{product} : q &= \dot{m} C_p \Delta T_{Reg}, \\ F_1 C_p \Delta T_{feed} + M_3 C_p \frac{\mathrm{d}T_{int3}}{\mathrm{d}t} &+ Q_{loss2} = F_2 C_p \Delta T_{Reg}, \end{aligned} \tag{3.20}$$

where $\Delta T_{feed} = T_{in} - T_a$ is the variation temperature between the output and input product flow. Moreover, M_3 is the mass product inside the regeneration phase and $\frac{\mathrm{d}T_{int3}}{\mathrm{d}t}$ is the variation of the internal mean temperature of the product in the regeneration phase $\left(T_{int3} = \frac{T_a + T_{in}}{2}\right)$. Finally, $\Delta T_{Reg} = T_1 - T_3$ is the different temperature of water between the input and output flow.

To calculate (M_3), the internal volume of the regeneration phase (49.68 cm^3) and the density of the product are considered, i.e, 49.7 g.

As explained before, the heat exchanger is not isolated therefore a heat loss to the environment Q_{loss2} should be contemplated. Figure 3.15 shows that the heat loss do not seem to be related with the speed of the feeding pump N_1 or the temperature T_1 and can be approximated to a constant value of 44 W.

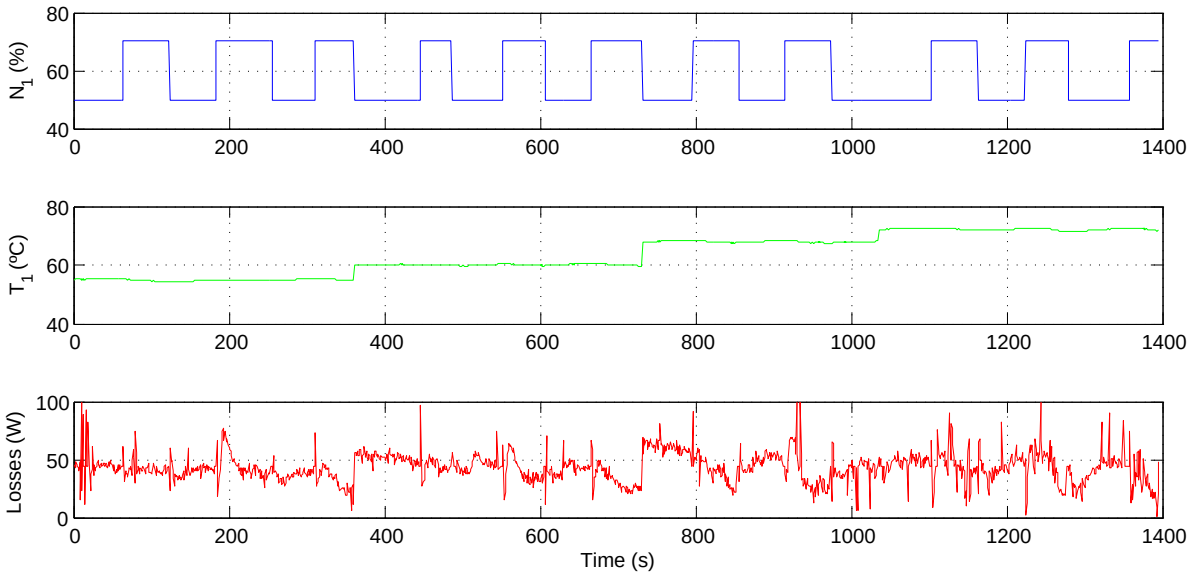

Figure 3.15: Evolution of the N_1, T_1 and losses of the regeneration phase

The losses are added to the equation 3.20, in the following way:

$$F_1 C_p \Delta T_{feed} + M_3 C_p \frac{\mathrm{d}T_{int3}}{\mathrm{d}t} + 44 = F_1 C_p \Delta T_{Reg}. \tag{3.21}$$

3.6 Model validation

In order to validate the resulting models, real data from the pasteurization plant has been extracted. To evaluate the comparison between the model-obtained temperatures and the real system temperatures, the Key Performance Indicator (KPI) will be calculated [KR03] using the expression:

$$KPI_i = \sqrt{\frac{1}{N}\sum_{k=1}^{N}(r_i(k) - z_i(k))^2}, \tag{3.22}$$

where N is the number of samples, $r_i(k)$ the real temperature of the variable i at the instant k, $z_i(k)$ the temperature of the variable i at the instant $k = t$ calculated by the continuous model. Finally i is the variable evaluated and k the instant studied.

The software PCT23 allows extracting data in steps of time higher than 1 s. Based on previous studies with the same small-scale plant, a sampling time of 1 s has been selected to validate the model [ROM15] [Cai12].

The validation process proposed has been divided in two steps based on changes on of the different actuators.. The first one step takes the first 250 s and N_1, N_2 and P have been set at 30 %, 30 % and 220 W, respectively. During the second steps the actuators values have been set at 50 % for N_1, 40 % for N_2 and 422 W for P.

The first element validated using integrated approaches is the hot-water tank. With this methodology the temperature T_2 or T_{2r} can be calculated knowing the value of the other variables. The lectures of the power have not been constants, fluctuating around the power value stablished, consequently, a filtrate method has been applied. The powers values resulted after the filtration have been 220 and 422 W.

Evolution of temperature T_2 obtained from experimental data and hot-tank model proposed with 3.11 is presented Figure 3.16. KPI has a value of 0.23 °C representing a relative error less than 1 %.

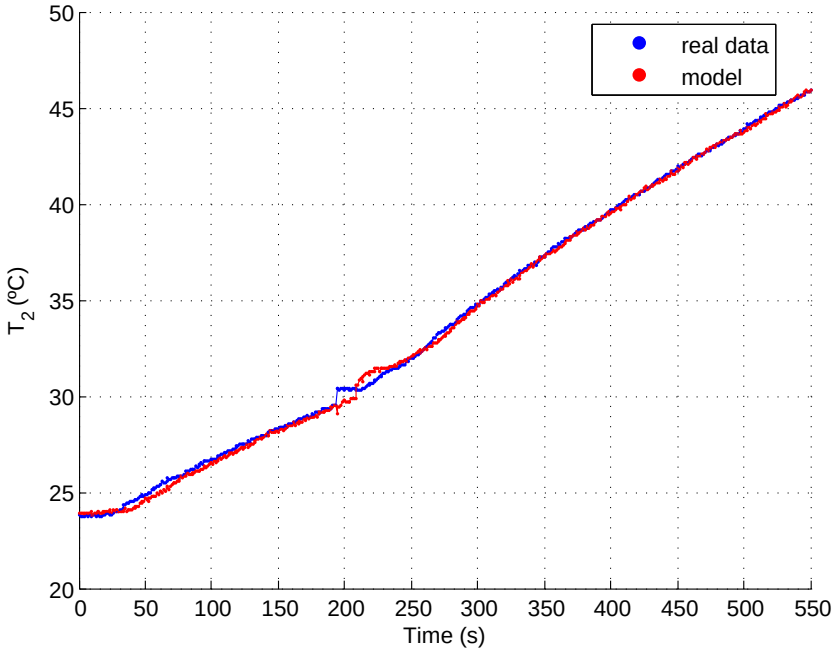

Figure 3.16: Evolution of T_2 in the hot-water tank

The second element that has been verified is the holding tube. The temperature T_1 (output of the element) has been calculated knowing the value of the actuator N_1 and the variables T_4 and T_a. Figure 3.17 shows that the model-obtained temperature (red line) follows the validation data of T_1 (blue line). The KPI is 0.20 °C representing less than a 1 % of error.

As mention in the section 3.5, the heat exchanger has three phases but only two have been modelled. Figure 3.18 presents the evolution of the output liquid temperature T_4 obtained experimentally (blue line) and using the models 3.21 and 3.19 (red line). The model fits the experimental data at different conditions however it is no able to describe T_4 during an actuators changes as can be seen between 200 and 250s. The KPI obtained is 0.45 °C representing less than a 2 % of error.

Briefly, Table 3.1 summarizes all KPI indicators from to the dynamic models pro-

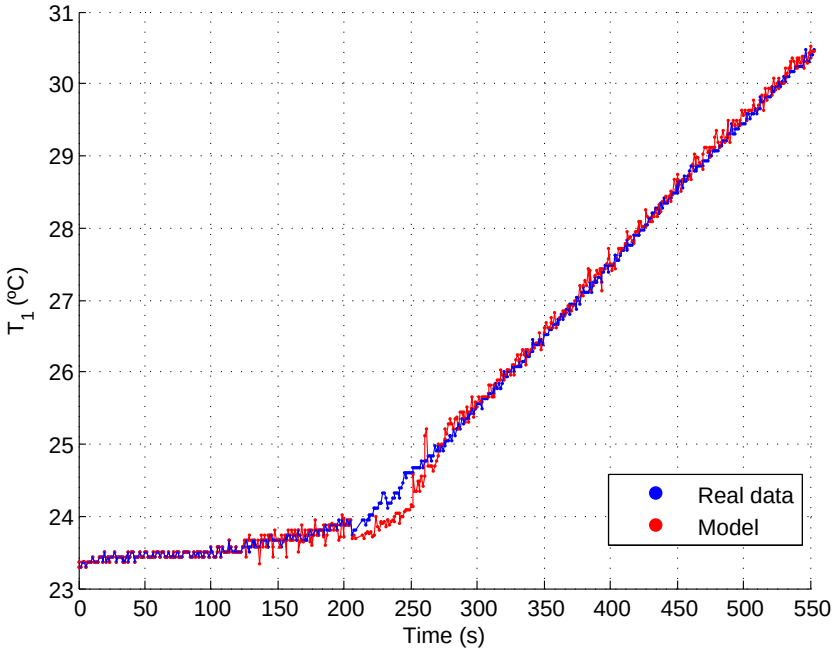

Figure 3.17: Evolution of T_1

posed in the current chapter.

Table 3.1: Summary of the performance according to the KPI

Element	Temperature	KPI
Hot-water tank	T_2	0.23 °C
Holding tube	T_1	0.20 °C
Heat exchanger	T_4	0.45 °C

Analysing the results, the higher value of KPI is lower than 0.5 °C. Taking into account the range of temperatures that represents a relative error between a 1.5 and 2 %. These values indicate that the model obtained approaches the data of the real small-scale pasteurization plant.

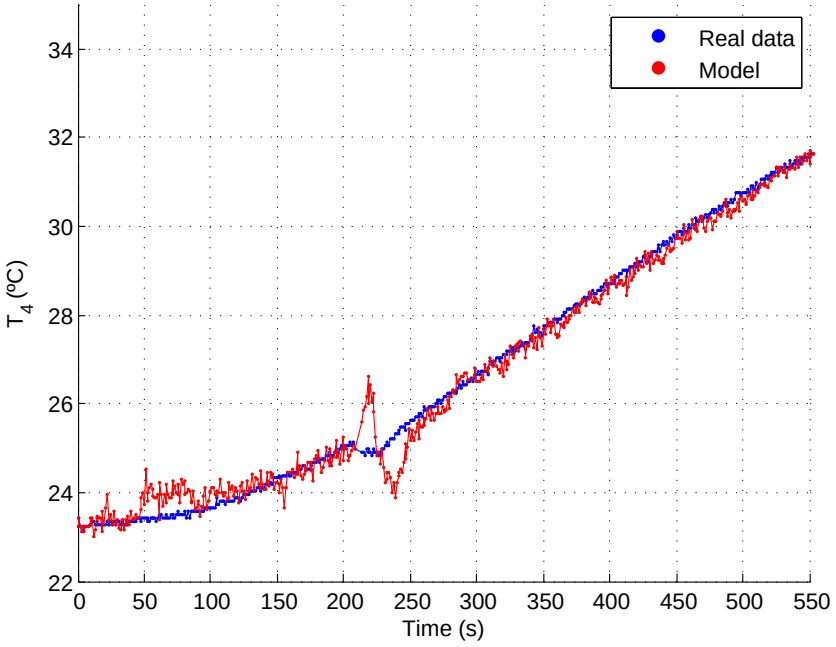

Figure 3.18: Evolution of T_4

Finally, Figure 3.19 shows the evolution of the variables T_2, T_4 and T_1 obtained from the experimental plant and model-obtained. Also changes on the actuators during the period studied are depicted.

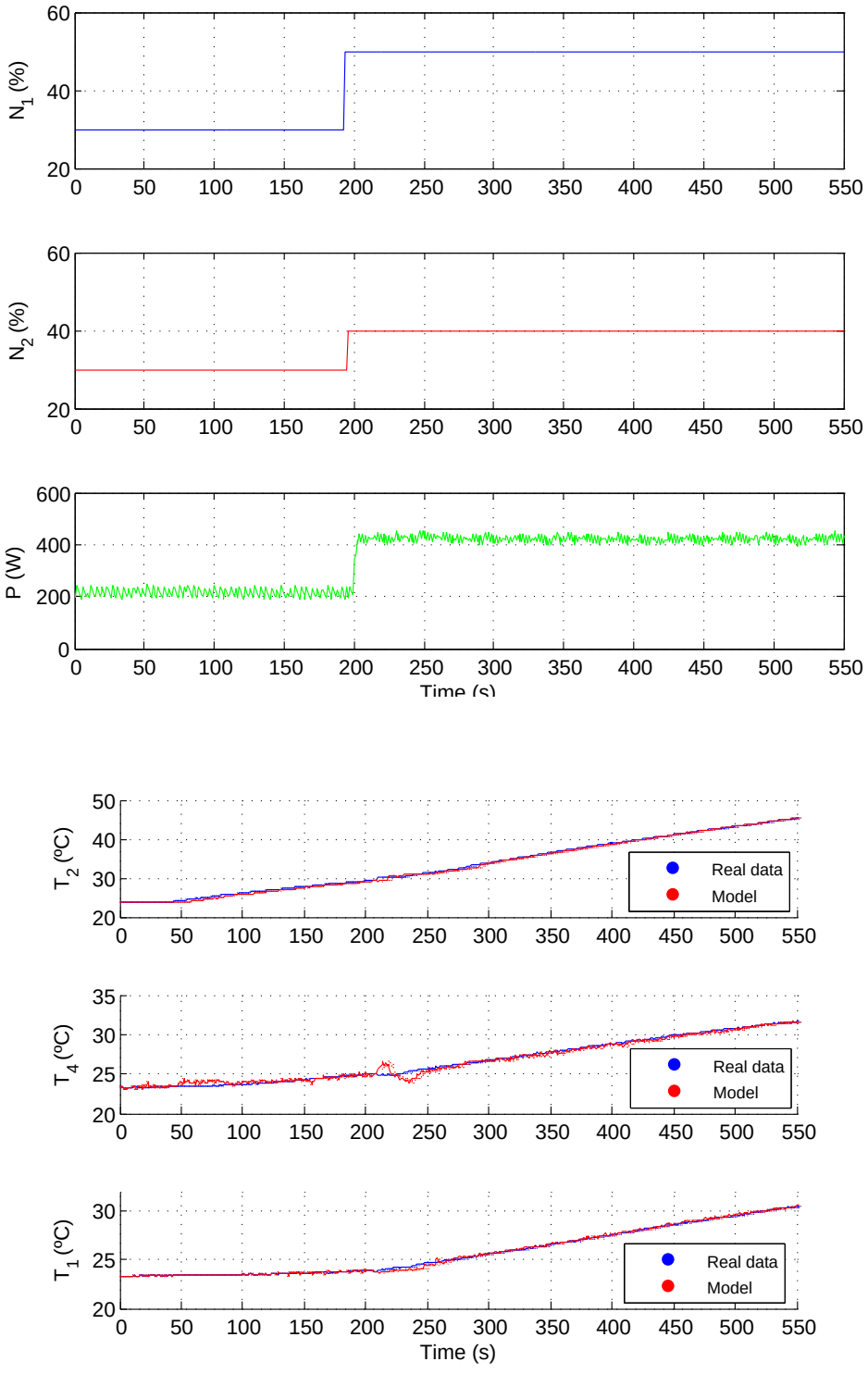

Figure 3.19: Inputs and outputs of the system

Chapter 4

LPV modelling

Linear Parameter-Varying (LPV) system [Sha12] is a linear state-space model whose dynamics change as a function of certain exogenous nonstationary parameters called scheduling parameters, expressed as:

$$\begin{aligned} \dot{x} &= A(\psi)x + B(\psi)u, \\ y &= C(\psi)x, \end{aligned} \tag{4.1}$$

where u is the input, y is the output, x is the vector of state variables, $\dot{x}$ the derivative of the state and ψ is an exogenous parameter vector that can be time dependent. It is assumed that the scheduling parameters can be measure on-line.

Briefly, a LPV model can be defined as a family of linear models where each one represents the local behavior of a nonlinear plant. The LPV model of a nonlinear plant can be obtained from the physical equation by means of Jacobian linearization around a family of working points parametrized. This approach is called linearization scheduling [CPR12]. In this chapter a family of linear models has been developed and then a LPV model has been defined.

4.1 Family of linear local models

The nonlinear models proposed in Chapter 3 have been linearized around several working points in order to create a family of linear state-space models [Kha02]. Working points selected should accomplish two main conditions due to the pasteurization process.

The first one is that the temperature T_1 (Figure 2.1) should be around the pasteurization temperature and the second one refers to the time that the product maintains this temperature in the holding tube. With these two conditions the points have been chosen to cover all the operation range of a HTST (High Temperature Short Time) pasteurization process. To determinate the steady values of each variable on the working points, different constant values of the actuators N_1, N_2 and P have been applied until the plant has achieved the steady state. Moreover, the delay of the holding tube represents the period of time required for the pasteurization process.

The linearized models are presented by the state-space matrices A_i, B_i and C_i and their ranges depend on the delay. In order to have always the same matrix range, in this project the pasteurization time has been considered fixed by feeding pump speed N_1 that means a constant flow F_1.

By 3.12, the value of the feeding pump speed N_1 has been calculated considering the typical pasteurization time ranged between 15-25 s. Finally, a delay or pasteurization time of 23 s has been proposed with a N_1 of 70 %.

Table 4.1 reports the different values of the sensors and actuators at the steady state of each working point.

In order to have a discrete model, the sampling time T_s has been defined. The sampling time chosen is 1 s, the same value proposed in previous studies related with the small-scale pasteurization plant [ROM15] [Cai12].

Table 4.1: Variable values at each operation point

Operation Points	$N_1(\%)$	N_2 (%)	P (W)	T_1 (°C)	T_2 (°C)	T_3 (°C)	T_4 (°C)
Operation Point 1	70	50	340	45.70	65.33	35.93	46.20
Operation Point 2	70	70	356	49.58	63.13	37.94	50.10
Operation Point 3	70	80	405	53.25	66.58	39.92	53.98
Operation Point 3	70	80	495	60.06	76.17	43.37	60.86

In order to verify this sampling time, the model of the element with the lower time constant T (heat exchanger) has been studied. An empirical rule to select T_s propose that the maximum value of T_s can be determined as a tenth part of the time constant T [LMB03]. Figure 4.1 shows the step response for the transfer function of the heat exchanger. As can be seen in the Figure, the static gain K is 0.7825 °C therefore the time constant T (time required to achieve a value of $0.632K$) is 10.7393 s. and settling time ts (time required to achieve a value of 0.95K) of 30 s and. Applying the empirical rule described before, the sampling time should be lower than 1.07 s. Consequently, 1 s can be employed. In order to develop the state-space model of the real plant, two parts have been distinguished. The first one includes the hot-water tank and the heat exchanger and teh second one the holding tube.

4.1.1 Hot-water tank and heat exchanger state-space model

The Jacobian linearization based on Taylor series has been applied to the equations presented in chapter 3 in order to develop a family of local linear models that approximates the data of the process around the linearization point [LRV05].

The return temperature of the hot-water T_{2r} and the temperature T_in are not motorized in the experimental plant. Their values are determined by the following expressions:

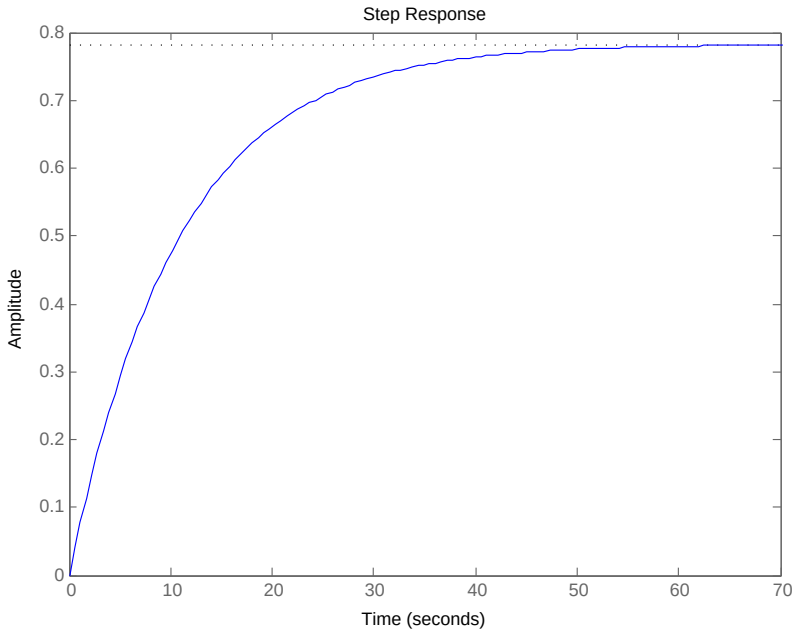

Figure 4.1: Evolution of the temperature T_4 and T_1

$$\begin{aligned} T_{2r} &= T_4 - a. \\ T_{in} &= T_3 - b. \end{aligned} \tag{4.2}$$

where a and b are constants at each working point. Substituting 4.2, the nonlinear equations change into:

$$\begin{aligned} F_1 &= \frac{\mathrm{d}T_2}{\mathrm{d}t}, \\ &= \frac{P}{7524} - \frac{0.4}{7524}(N_2 - 20)(T_2 - T_4 + a) - \frac{1.20}{7524}(T_2 - T_a), \end{aligned} \tag{4.3}$$

$$F_2 = \frac{\mathrm{d}T_3}{\mathrm{d}t}, \\ = \frac{1}{M_4 C_p}\left(\frac{4.1120(N_1-20)C_p(T_3-b-T_a)}{60} + 44 - \frac{4.1120(N_1-20)C_p(T_1-T_3)}{60}\right), \tag{4.4}$$

$$F_3 = \frac{\mathrm{d}T_4}{\mathrm{d}t}, \\ = \frac{2}{M_2 C_p}\left(\frac{11.1187(N_2-20)(T_2-T_4+a)}{60} - \frac{4.1120(N_1-20)C_p(T_4-T_3+b)}{60} - \right. \\ \left. (0.135N_1 - 0.499)(T_2-27) - \frac{\mathrm{d}T_{in}}{\mathrm{d}t}, \right. \tag{4.5}$$

$$F_4 = \frac{\mathrm{d}T_{in}}{\mathrm{d}t}, \\ = \frac{1}{M_3 C_p}\left(\frac{4.1120(N_1-20)C_p(T_1-T_3)}{60} - 44 - \frac{4.1120(N_1-20)C_p(T_3-b-T_a)}{60}\right), \tag{4.6}$$

Applying the Jacobian linearization to 4.3, 4.4 and 4.5 the continuous linearized state-space model around the working point i has the following structure:

$$\begin{pmatrix} \frac{\mathrm{d}T_{2\delta}(t)}{\mathrm{d}t} \\ \\ \frac{\mathrm{d}T_{3\delta}(t)}{\mathrm{d}t} \\ \\ \frac{\mathrm{d}T_{4\delta}(t)}{\mathrm{d}t} \\ \\ \end{pmatrix} = A_{Ai} \begin{pmatrix} T_{2\delta}(t) \\ T_{3\delta}(t) \\ T_{4\delta}(t) \end{pmatrix} + B_{Ai} \begin{pmatrix} N_{1\delta}(t) \\ N_{2\delta}(t) \\ P_{\delta}(t) \end{pmatrix} \\ y(t) = C_{Ai} \begin{pmatrix} T_{2\delta}(t) \\ T_{3\delta}(t) \\ T_{4\delta}(t) \end{pmatrix} \tag{4.7}$$

where $T_{2\delta}$, $T_{3\delta}$, $T_{4\delta}$, $N_{1\delta}$, $N_{2\delta}$ and P_{δ} are the incremental values around the operating points of the states and inputs. Matrices A_{Ai}, B_{Ai} and C_{Ai} are expressed as:

$$A_{Ai} = \begin{pmatrix} \frac{\delta F_1(t)}{\delta T_2}_{OP_i} & \frac{\delta F_1(t)}{\delta T_3}_{OP_i} & \frac{\delta F_1(t)}{\delta T_4}_{OP_i} \\ \frac{\delta F_2(t)}{\delta T_2}_{OP_i} & \frac{\delta F_2(t)}{\delta T_3}_{OP_i} & \frac{\delta F_2(t)}{\delta T_4}_{OP_i} \\ \frac{\delta F_3(t)}{\delta T_2}_{OP_i} & \frac{\delta F_3(t)}{\delta T_3}_{OP_i} & \frac{\delta F_3(t)}{\delta T_4}_{OP_i} \end{pmatrix}$$

$$B_{Ai} = \begin{pmatrix} \frac{\delta F_1(t)}{\delta N_1}_{OP_i} & \frac{\delta F_1(t)}{\delta N_2}_{OP_i} & \frac{\delta F_1(t)}{\delta P}_{OP_i} \\ \frac{\delta F_2(t)}{\delta N_1}_{OP_i} & \frac{\delta F_2(t)}{\delta N_2}_{OP_i} & \frac{\delta F_2(t)}{\delta P}_{OP_i} \\ \frac{\delta F_3(t)}{\delta N_1}_{OP_i} & \frac{\delta F_3(t)}{\delta N_2}_{OP_i} & \frac{\delta F_3(t)}{\delta P}_{OP_i} \end{pmatrix}$$

$$C_{Ai} = \begin{pmatrix} 1 & 1 & 1 \end{pmatrix}$$

where $OP_i = \{N_{1opi}, N_{2opi}, P_{opi}, T_{1opi}, T_{2opi}, T_{3opi}, T_{4opi}, T_{4opi}, a_{opi}, b_{opi}\}$ are the values of actuators and variables at the steady state of the working point i.

The continuous state-state model has been transformed to discrete-time using a sampling time T_s of 1 s. The new matrices are given by:

$$\begin{aligned} A_{Adi} &= e^{A_{Ai}T_s}, \\ &= A_{Ai}T_s + I, \\ B_{Adi} &= \left(\int_0^{T_s} e^{A_{Ai}\tau} d\tau \right) B_{Ai)}, \\ &= T_s B_{Ai}. \end{aligned} \tag{4.8}$$

Finally, the discrete state-space can be defined as:

$$\begin{aligned} x_A(k+1) &= A_{Adi}x_A(k) + B_{Adi}u_A(k), \\ y_A(k) &= C_A x(k). \end{aligned} \tag{4.9}$$

The final values of the matrices are presented in Appendix A. The matrices have been found by using Maple software (see Appendix C).

4.1.2 Holding tube state-space model

The holding tube is the element of the plant that presents a delay. As mentioned before, the delay has been fixed at 23 s. The resulting linearized model can be expressed by the following transfer function:

$$\begin{aligned} G_{T1}(s) &= \frac{T_{1\delta}(s)}{T_{4\delta}(s)}, \\ &= \frac{0.08285e^{-23s}}{s + 0.08430}. \end{aligned} \tag{4.10}$$

Applying a sampling time of 1 s,the discrete transfer function can be expressed as:

$$\begin{aligned} G_{T1}(z) &= \frac{T_{1\delta}(z)}{T_{4\delta}(z)}, \\ &= \frac{0.07946z^{-23}}{z - 0.91920}. \end{aligned} \tag{4.11}$$

By the Matlab function *ss* the state space of the transfer function has been found, resulting the following expression:

$$\begin{aligned} x_B(k+1) &= A_B x_B(k) + B_B u_B(k), \\ T_{1\delta}(k) &= C_B x_B(k), \end{aligned} \tag{4.12}$$

where u_B(k) = $T_{4\delta}$ (k) is the input, $x_B \in \Re^{24}$ is the state vector and $A_B \in \Re^{24x24}$, $B_B \in \Re^{24}$, $C_B \in \Re^{1x24}$. The matrices A_B, B_B and C_B have always the same value because the linearization only depends on N_1 which has a fixed value (see the final values at Appendix B).

4.1.3 Final linearized model

The final model involves the two models developed in series, first, hot-water tank and heat exchanger model and then the holding tube model. This proposal is based on the fact that the values of the matrices of the holding tube model are constant and do not depend on the working point. Figure 4.2 shows the scheme of the final model. The

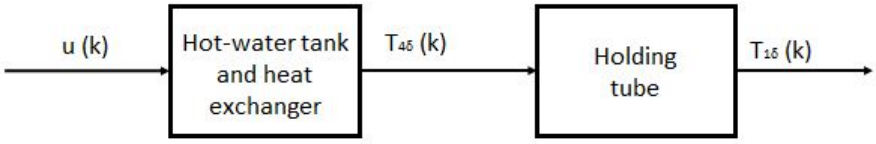

Figure 4.2: Final model scheme

inputs $u(k)$ are $N_{1\delta}$, $N_{2\delta}$ and P_δ and the final output is the temperature $T_{1\delta}$. The output of the first model is $T_{4\delta}$ also the input of the second model, therefore the matrix C of the first model 4.12 changes into:

$$C_{Ai} = \begin{pmatrix} 0 & 0 & 1 \end{pmatrix}$$

4.2 LPV model

Matrices of the state equation of hot-water tank and heat exchanger, presented in section 5.1, depend on varying parameters. Therefore, a first approach of a LPV model for these elements is developed in this section.

As a first approach the matrix $B_{Ai}(\psi(k))$ has been considered invariant. This is based on working at fixed speeds around each operating point. The incremental inputs $N_{1\delta}$ and $N_{2\delta}$ at this conditions are nulls. Therefore, only the state matrix A_{Ai} depends on varying parameter $\psi(k) = \ N_2(k)\ $ that is measurable [DR13].

The state-space model depends on the parameter in a polytopic manner[RNP13], hence the LPV model created is polytopic, i.e.,

$$A(\psi(k)) = \sum_{j=1}^{N} \pi_j(\psi(k)) A_j, \tag{4.13}$$

with $\sum_{j=1}^{N} \pi_j(\psi(k)) = 1$ and $\pi(\psi(k)) \geq 0$ where where N is the number of vertex, π_j is the polytopic coordinate of the vertex j and A_j the state-space matrix at that vertex.

By considering the lower and upper bounds of element in $\psi(k)$ for speed ranges [50 %, 80 %] and taking each permutation, 2 vertex models are formed [DR13]. See vertix matrix at Appendix C. As having only 2 vertex, the polytopic coordinate for the lower and upper bound, respectively will be calculated as:

$$\begin{aligned} \pi_1(\psi(k)) &= \frac{\psi_{max} - \psi(k)}{\psi_{max} - \psi min}, \\ \pi_2(\psi(k)) &= 1 - \pi_1(\psi(k)). \end{aligned} \tag{4.14}$$

The final LPV model obtained for the hot-water tank and the heat exchanges can be expressed as:

$$\begin{aligned} x_A(k+1) &= \sum_{j=1}^{N} \pi_j(\psi(k)) A_j x_A(k) + B_A u_B(k), \\ T_{4\delta}(k) &= C_B x_A(k), \end{aligned} \tag{4.15}$$

The model has been simulated in the 4 operating points. The values of polytopic coordinates calculated using 4.2at each working point are presented in Table 4.2:

Figure 4.3 shows the evolution of T_2, T_4 and T_1 around each operating point. The blue line represents the real data and the red line the temperatures obtained with the LPV model. The KPI obtained for each temperature are 1.25 °C, 1.25 °C and 1.06 °C for T_2, T_1 and T_4, respectively.

Table 4.3 shows the comparison of the relative error for the nonlinear model (called

Table 4.2: Values of the π_j at each working point

operating point	π_1	π_2
OP_1	1	0
OP_2	0.333	0.666
OP_3	0	1
OP	0	1

model 1) and the LPV model in series with the holding tube space-state model (model 2).

Table 4.3: Comparison of the relative errors

Element	Temperature	Error Model 1	Error Model 2
Hot-water tank	T_2	0.6-1 %	1.6-2 %
Holding tube	T_1	0.5-1 %	2-2.8 %
Heat exchanger	T_4	1.5-2 %	1.7-2.4 %

Model 1 presents a lower relative errors for all the elements compared with the second model but in both cases lower than 3 %.

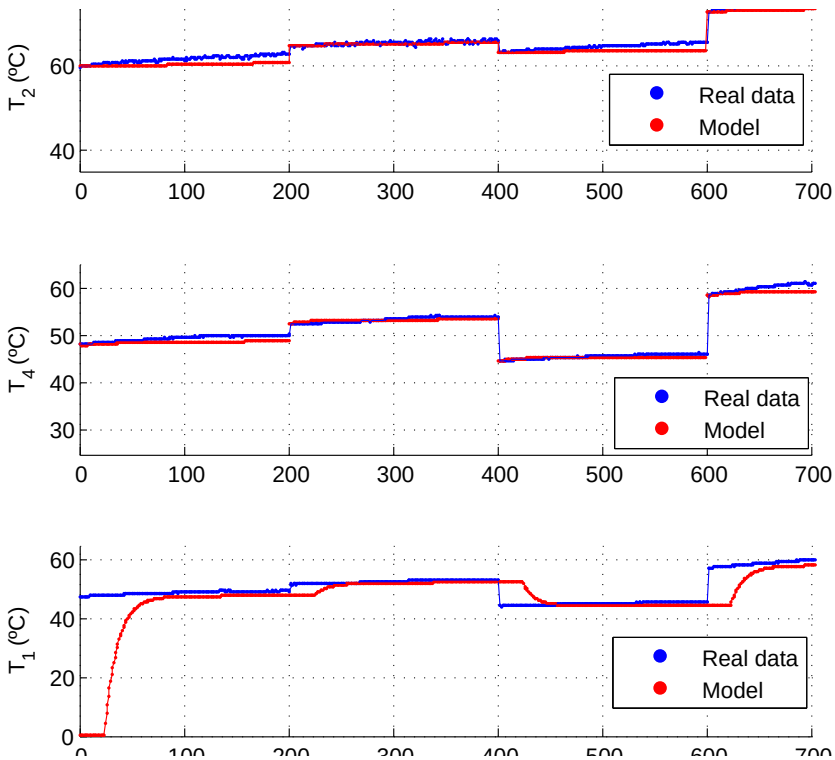

Figure 4.3: Evolution of the T_2, T_4 and T_1

Chapter 5

PID control design and simulation

The pasteurization plant presents some perturbations that affect the overall performance. Further, changes in one variable influences to the other ones. Hence, it is important to design a controller to reach the goals of the process. Although this work has been focused on the development of a model for the plant,a control strategy using a PID controller has been designed and simulated as a first approach [ROM15] [WWM12].

A PID (Proportional-Integral-Derivative) controller is a control mechanism that works with a feedback loop. It calculates the error (e) between the output (y) and the desired value (r) in order to apply a control action (u) that fits in the process. Figure 5.1 shows a scheme of the PID control loop where G represents the transfer function of the plant [Kuo96] [Oga95]. Moreover, the discrete transfer function of a PID controller that relates the input u(z) with the error e(z) can be expressed as:

$$G_{PID}(z) = K_P + \frac{K_I}{1 - z^{-1}} + K_D(1 - z^{-1}), \tag{5.1}$$

where K_P is the proportional gain, K_I the integral gain and K_D the derivative gain. In order to avoid the increase of the noise in the experimental plant, the derivative gain has been considered null. Taking into account this consideration a control loop for each

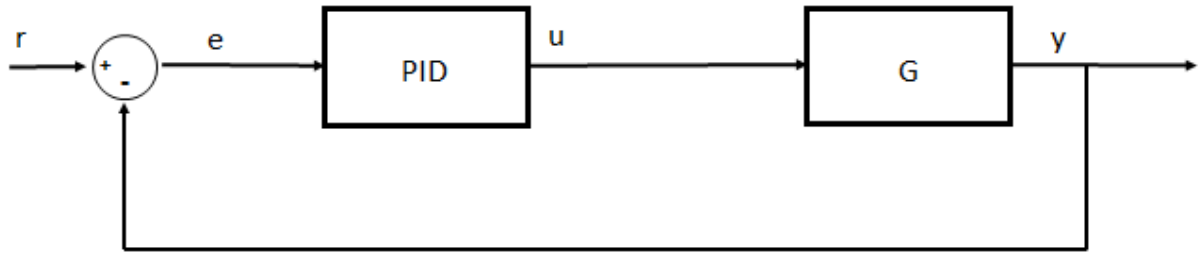

Figure 5.1: Scheme of the PID control loop

variable has been created.

The inputs of the smalls-scale pasteurization plant are the speed of the pumps N_1 and N_2 and the power P of the electrical resistor while the measured outputs are the flow F_1 and the temperatures T_1, T_2, T_3 and T_4. For each output parameter, a control loop is designed, except for T_3 as it has not been controlled. A brief description of each control loop is exposed in the following points:

- Flow F_1 controlled by the speed of the pump N_1: One of the goals of a pasteurization plant is the time that the product remains at certain temperature. This time can be fixed controlling the flow rate through the holding tube. As proposed in chapter 4, the present study uses a fixed value of 23 s by setting the speed of the speed of the feeding pump N_1 at 70 %. Notice that is a feed-foward control.

- Temperature in the hot-water tank T_2 through the power of the electrical resistor P (Figure 4.5): The hot-water is the thermal energy source used to heat the product. To a proper system operation, T_2 must always be greater than T_1 and T_4 and enough to achieve the final temperature desired. Therefore, a controller for this temperature should be designed in order to guarantee the energy for the process.

- Temperature of the product T_1 through the temperature at the output of the heating phase of the exchanger T_4 (Figure 4.6): The temperature T_1 (output temperature of the holding tube) must be the pasteurization temperature stablished in the process.

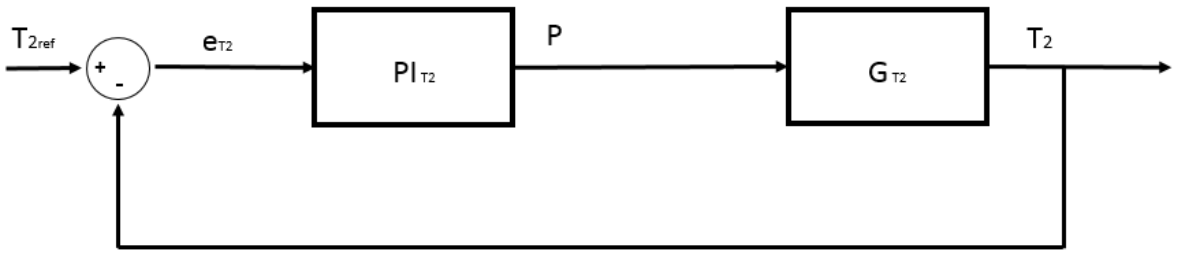

Figure 5.2: Scheme of the temperature T_2 control

It depends on T_4 that is controlled by the speed of the hot-water pump N_2. The T_1 control loop proposed is in series [Val95] as presented in Figure 4.6.

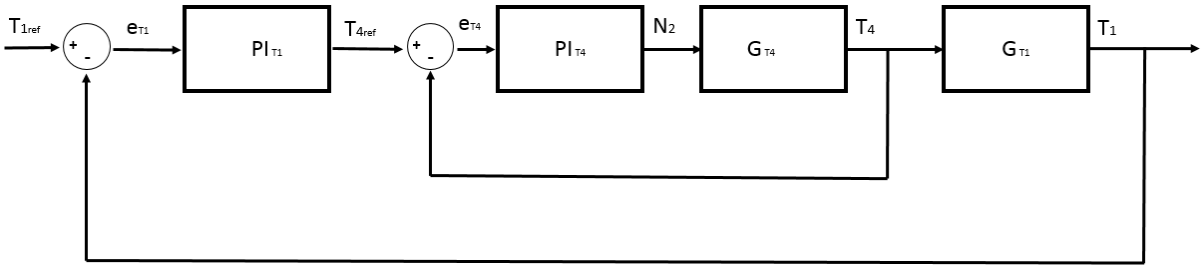

Figure 5.3: Scheme of the temperature T_1 control

The controller has been designed for a linearized model that works around one of the operating points stablished in the Chapter 4. The selected working point is characterized by N_1 of 70 % (that represents a flow of 205 ml/min), N_2 of 80 % (higher values could deteriorate the pumps) and a power P of the electrical resistor of 405 W. This power is high enough to reach a temperature T_1 close to 55 [∘C. The operating temperatures with these actuators values are presented in Table 4.4:

The PI controller designed should permit to reach the reference temperature proposed without oscillations. Moreover, the settling time has also to be considered. The faster the desired temperature is reached the fewer product will not be pasteurized. To design these PI controllers, MATLAB tool *sisotool* has been used.

Table 5.1: Value of the temperatures at the working point

Variable	Description	Value (°C)
T_1	Temperature of the product at the output of the holding tube	53.25
T_2	Temperature of the hot-water	66.58
T_3	Temperature of the final product	39.92
T_4	Temperature of the product at the output of the heat exchanger	53.98

5.1 Control of the temperature T_2

In this section a PI controller is designed in order to regulate the water temperature of the hot-water tank T_2. This temperature may be maintained at a certain constant and high value to guarantee enough energy to be transferred to the product. Therefore, T_2 should be around 66.58 ° (Table 4.4) as it has been determined experimentally. The controller will act over the electrical resistor power P.

The model of the hot-water tank is described with the nonlinear equation 3.11 based on physical principles. The linearization around the working point has been done with the Taylor series as in [Kuo96]:

$$\frac{\mathrm{d}x_\delta}{\mathrm{d}t} = \frac{\delta f}{\delta x}_{P_0} + x_\delta + \frac{\delta f}{\delta y}_{P_0} y_\delta, \tag{5.2}$$

Considering $x_\delta = T_{2\delta}$, $y_\delta = P_\delta$ and $f = \frac{\mathrm{d}T_{2\delta}}{\mathrm{d}t}$ isolated from (3.11), 4.17 can be written as

$$\frac{\mathrm{d}T_{2\delta}}{\mathrm{d}t} = \left(\frac{-k_1}{C_A}(N_2 - 20) - \frac{k_2}{C_A}\right) T_{2\delta} + \frac{1}{C_A} P_\delta. \tag{5.3}$$

After applying the Laplace transform, the transfer function that relates $T_{2\delta}$(s) and P_δ(s)

has been found

$$\begin{aligned} G_{T2}(s) &= \frac{T_{2\delta}(s)}{P_{\delta}(s)}, \\ &= \frac{\frac{1}{C_A}}{s - \left(\frac{-k_1}{C_A}(N_2 - 20) - \frac{k_2}{C_A}\right)}, \\ &= \frac{0.0001329}{s + 0.002824}. \end{aligned} \tag{5.4}$$

The discretization of all dynamics is performed using the sampling time of 1 s found in Chapter 4. The transfer function of the hot-water tank G_{T2}, Matlab function $c2d$ has been used, i.e.,

$$G_{T2}(z) = \frac{0.0001327}{z - 0.9962}. \tag{5.5}$$

The PI gains values have been determined considering that the system reaches the desired temperature of 66 °C without oscillations in the response and reducing the settling time. The values of the proportional gain K_{P1} and integral gain K_{I1} that satisfies the control objective are presented in Table 4.5.

Table 5.2: Values of the PI controller gains for the T_2 control loop

Parameter	Value
K_{P1}	382.8120
K_{I1}	2.6644

Figure 4.7 represents the evolution of the temperature T_2 using the PI controller to achieve a desire temperature of 66 °C. Using the PI controller, the system reaches the desired temperature with a lower settling time (240 s) compared to the open loop (1100 s). Also it has a smooth overshoot that represents percentage of a 5 %.

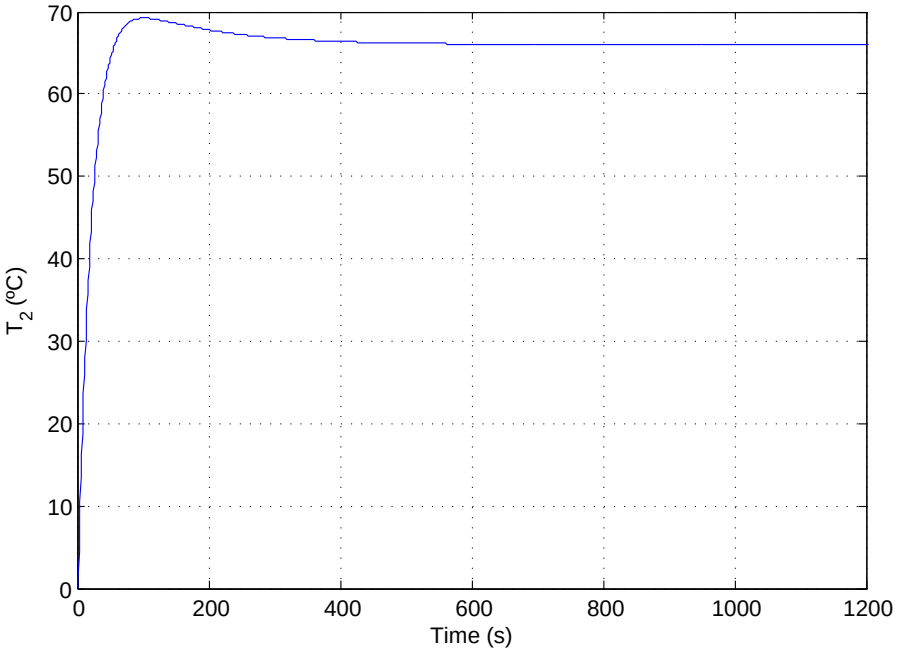

Figure 5.4: Scheme of the temperature T_2 control

5.2 Control of the temperature T_4

The temperature T_4 is the temperature of the product at the output of the heating phase of the heat exchanger. The linearization has been done with the Taylor series as in the section 5.1. and the input has been considered the speed of the hot-water pump N_2. Applying the linearization and Laplace transform to 3.19 the transfer function can be expressed as:

$$\begin{aligned} G_{T4}(s) &= \frac{T_{4\delta}(s)}{N_{2\delta}(s)}, \\ &= \frac{0.07287}{s + 0.09312}. \end{aligned} \tag{5.6}$$

Being the sampling time of 1 s and using $c2d$ Matlab function, the discrete transfer function obtained from 4.21 is:

$$G_{T4}(z) = \frac{0.0.06958}{z - 0.91110}. \tag{5.7}$$

The design parameters of this control loop are to reach the reference without overshoots and to have a settling time lower than 10 s. Table 4.6 presents the values of the proportional and integral gains that achieve the design conditions.

Table 5.3: Values of the PI controller gains for the T_4 control loop

Parameter	Value
K_{P2}	7.6348
K_{I2}	0.6941

Figure 4.8 presents the simulation with the PI controller implemented. It reaches the desired temperature of 54 °C with a settling time of 7.25 s (lower than the open loop that was 10.1 s) and remains constant during all the period.

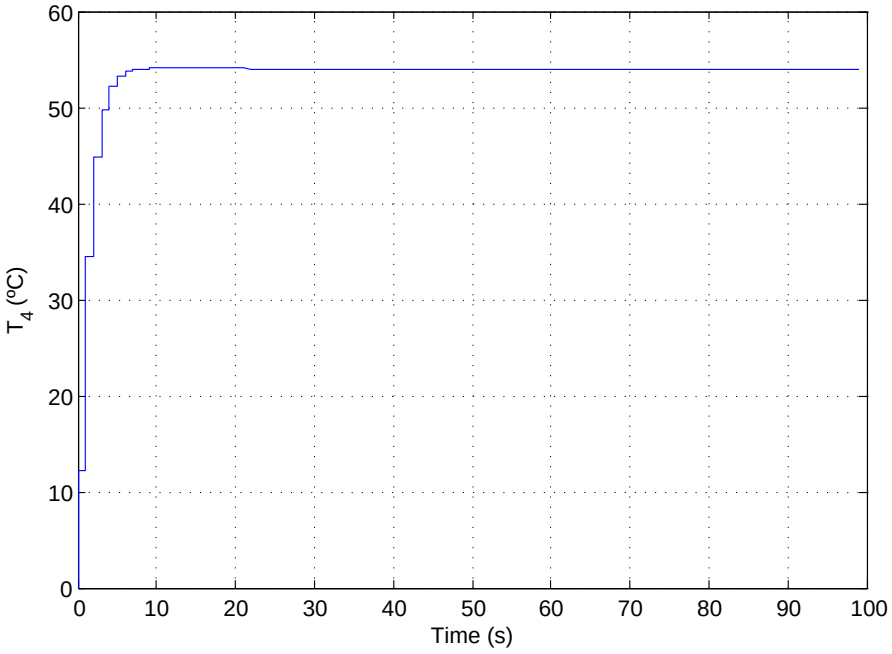

Figure 5.5: Evolution of the T_4 applying the PI controller

5.3 Control of the temperature T_1

The temperature T_1 is the most important temperature of the plant as it indicates if the product is pasteurized or not. Its control is in series as presented in Figure 4.6 The function transfer from the holding tube model 3.16 relates $T_{1\delta}$ with $T_{4\delta}$ as described in the following equation:

$$\begin{aligned} G_{T1}(s) &= \frac{T_{1\delta}(s)}{T_{4\delta}(s)}, \\ &= \frac{0.08285\exp^{-23s}}{s+0.08430}. \end{aligned} \tag{5.8}$$

Applying *c2d* Matlab function and the sampling time of 1 s, the discrete function transfer can be obtained, i.e.,

$$G_{T4}(z) = \frac{0.07946z^{-23}}{z-0.9192}. \tag{5.9}$$

The main objective of controlling the temperature T_1 is to achieve the pasteurization temperature without oscillations or considerable overshoot. In the Table 4.7 are reported the gains of the PI controller that accomplish the design characteristics.

Table 5.4: Values of the PI controller gains for the T_1 control loop

Parameter	Value
K_{P2}	0.1500
K_{I2}	0.0155

Figure 4.9 shows the evolution of T_1 using the PI controller designed. It has a delay of 23 s but then the desired temperature is reached with a settling time of 150 s. The evolution presents a smooth overshoot of a 1.9 %.

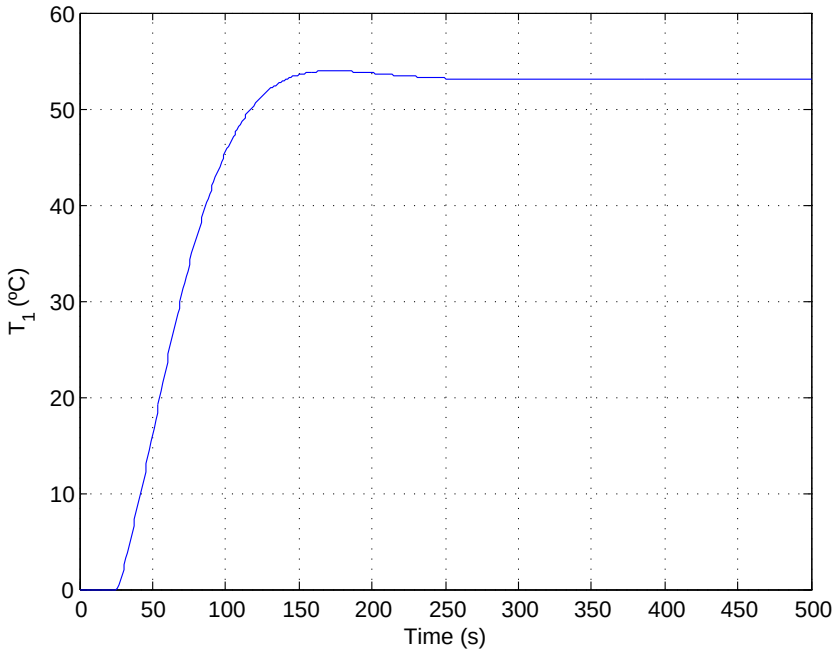

Figure 5.6: Evolution of the T_1 applying the PI controller

Chapter 6

Environmental impact

The term environment is used to indicate groups of people, ecosystems, goods, cultures, socio-economic structures, etc. that constitutes the operating framework, not only the environment intended as physical space.

Usually, small-scale home processing activities produce relatively small amounts of waste and waste water. Nature can cope with these. Yet as a consequence of the increasing emphasis on large scale production (e.g. for reasons of efficiency, increase in scale of production and hygiene) considerably greater amounts of waste will be produced and steps will have to be taken to keep this production at acceptable levels.

The small-scale pasteurization plant does not affect the environment with air pollution but the areas in witch the contents of this project can be applied is the production of noise pollution. Although the plant has a filtrate equipment to recycle the water there are some waste is produced.

Having a large scale production will have more environmental effects. There will be the waste milk (pure milk raw material mixed with water) in dairy wastewater coming from start-up and shutdown operations performed in the high-temperature, short time

(HTST) pasteurization process. In a large scale production a power resistor will be not enough to heat up the hot water used. So if a boiler if used then there will be air pollution due to the gasoil or coal used.

The advantage of using a control strategy to reach a pasteurization temperature is that extra energy will not be created. Knowing the power of resistor permits to heat until the exact point avoiding generating extra power therefore more air pollution.

Chapter 7

Budget evaluation

This chapter considers the budget to develop the present project considering the cost of the equipment and licences employed. Human resources cost associated such as technicians and directors have not been considered.

1. SOFTWARE	
Licence MatLab R2014a	1200
Licence Maple 18	0
Licence Texmarker 4.1	0
TOTAL SOFTWARE	1200
2. HARDWARE	
HP Pavilion dv6 Notebook Laptop	1200
Pasteurization plant PCT23 MKII	33000
64 bit Card 4.1	6000
TOTAL HARDWARE	40200
TOTAL BUDGET	41400

Chapter 8

Concluding remarks

8.1 Conclusions

In the present project two models for real-time control have been developed for a small-scale pasteurization plant PCT23 MKII. The experimental data has been acquired by the program ArmSoft PCT23 Process Plant Trainer for the parameter estimation and validation.

Concerning the nonlinear model based physical principles created, the following conclusions can be drawn:

- the dynamical model developed is based on physical principles. Moreover, nonlinear equations have been required to model the real plant;
- model validation presents mean quadratic error KPI lower than 0.5 °C with a relative error of 2 %;
- nonlinear system makes difficult to design a controller. Hence, a PID controller, based on SISO systems, have been designed and simulated. Despite the lineariza-

tion, this controller has demonstrated to reach the desired temperatures without oscillations or high overshoots.

Concerning the LPV model, the main conclusions are:

- LPV model for a wide operation temperature range is based on the nonlinear model;
- flow F_1 has been fixed to avoid changes on the delay and therefore on the matrices ranges;
- KPI has been calculated by means of experimental data. Values lower than 1.25 C have been obtained representing a relative error of 3 %;
- the LPV model has a higher relative error compared with the nonlinear model.

8.2 Contributions

The main contributions that have been made in this project are the following:

- Propose a nonlinear and dynamic model for the small-scale pasteurization plant. Each element of the plant has been modelled considering the physical process that take place. The constant parameters have been determined by means of experimental data acquired from the plant. The models have been validated by new experiments at different operation conditions.
- Develop a LPV model based on the nonlinear model. Considering the complexity of the nonlinear model developed a new linear model has been proposed. As the Jacobian linearization only allows working around one operating point a family of linear state-space models have been created. A final LPV model has been defined as the state-space matrix A_{Ai} is function of varying parameters.

- Design a PID controllers for a linearized model. For the desired performance of the plant, three different temperatures should be controlled. Therefore, a control loop for each one has been designed tanking into account the interconnections between element of the plant.

8.3 Further work

To continue the research related with this project, different ideas are outlined:

- Improve the nonlinear model. The model developed it able to fit experimental data at different conditions. However when there are changes on the actuators, the model is not able to take perfectly into account the two possible values during the integration time.

- Improve the PID controller. PID controller has been simulated in the linearized model therefore, a new goal could be implement it to the experimental plant and evaluate the system performance. Moreover, a redesign of the configuration taking into account the interrelation between temperature T_2 and T_4 .Also a PID controller including the derivative action can be designed and tested.

- Improve the state-space model by considering the changes of the delay. In this project the delay or pasteurization time has been fixed. As this parameter is one of the most relevant it should be taken into account in the state-space model. Therefore, matrix range will continuously change depending on the delay conferring complexity to the model.

- Improve the LPV model by considering a varying pump speeds. The LPV has been validated at fixed speeds hence, a new validation should be done varying the pump

speed during the validation. In this situation state-space matrices A_{Ai} and B_{Ai} will be functions of varying parameters.

- Consider the design of Model Predictive Control (MPC) based on the nonlinear model. MPC has the capability of handling multi-variable control problems taking into account actuator limitations and physical constraints [ROM15]. The design of a MPC controller would be the main goal of the future work.

Bibliography

[Arm10] Armfield. *Process Plant trainer PTC23-MKII.* Instruction Manual, 2010.

[CAGS99] M. De la Sen C.F. Alastruey and M. Garcia-Sanz. Modellng and identification of a high temperature short time pasteurization process including delays. *7th Mediterranean Conference on Control and Automation (MED99)*, pages 1890–1896, 1999.

[Cai12] Luis Caiza. *Disemplementacion de estatregias de control predictivo para una planta de pasteurizacion a escala.* UPC, 2012.

[DR13] V. Puig D. Rotondo, F. Nejjari. Quasi-lpv modeling, identification and control of a twin rotor mimo. *Control Engineering Practice*, 21, 2013.

[FBM15] G. Giordano F. Blanchini, D. Casagrande and S. Miani. On the lpv control design and its applications to some classes of dynamical systems. *Devepments in Model-Based Optimization and Control*, 464:319–332, 2015.

[HR04] David M. Himmelblau and James B. Riggs. *Basic Principles and calculations in chemical engineering.* Pearson Education, Inc., 2004.

[JCLA94] F. Cunill Garc. Esplugas Vidal C. Mans Teixido J. Costa Lopez, S. Cervera March and F. Mata Alvarez. *Curso de Ingenieruca.* RevertA, 1994.

[JIGS98] J.M. Sandoval J.J. Ibarrola, J.C. Guillen and M. Garcia-Sanz. Modelling of a high temperature short time pasteurization process. *Food Control*, 9:267–277, 1998.

[Kha02] Hassan K. Khalil. *Nonlinear systems*. Prentice Hall, Inc, 3 edition, 2002.

[KR03] Mohamed Tarek Khardir and John Ringwood. Linear and nonlinear model predictive control design for a milk pasteurization plant. *Control and Intelligent Systems*, 31, 2003.

[Kuo96] Benjamin Kuo. *Sistemas de Control Automco*. Prentice Hall, Inc, 7 edition, 1996.

[Lju87] Lennart Ljung. *System Identification: Theory for the User*. Prentice Hall, 1987.

[LMB03] Santiago Garrido Luis Moreno and Carlos Balaguer. *Ingeniere Control, Modelado y control de sistemas dincos.* Ariell S.A, 2003.

[LRV05] J. Bernussou L. Reberga, D. Henrion and F. Vary. Lpv modeling of a turbofan engine. *IFAC World Congress on Automatic Control*, 14, 2005.

[MGSI01] J.C. Guillen M. GarcSanz and J.J. Ibarrola. Robust controller design for uncertain systems with variable time delay. *Control Engineering Practice*, 9:961–972, 2001.

[MKO00] J Ringwood M.T. Khadir, J. Richalet and B. Oconnor. Modelling and predictive control of milk pasteurisation in a plate heat exchanger. *Proc. Foodsim*, 2000.

[Oga95] Katsuiko Ogata. *Discrete-Time Control Systems*. Prentice Hall, Inc, 2 edition, 1995.

[ROM15] A. Rosich and C. Ocampo-Martz. Real-time experimental implementation of predictive control schemes in a small-scale pasteurization plant. *Developments in Model-Based Optimization and Control*, 464:255–273, 2015.

[Sha12] Jeff S. Shamma. An overview of lpv systems. *Control of Liner Parameter Variying Systems with Applications*, 464:3–20, 2012.

[Val95] Joslderrama. *Simulaci procesos*. Centro de Informacicnola, 1995.

[VCR12] D. Piga V. Cerone and D. Regruto. Set-membership identification of input-output lpv with uncertain time-varying parameters. *Linear parameter-varying system identification*, 14, 2012.

[Wea98] Robert C. Weast. *CRC Handbook of chemistry and physics*. CRC Press, Inc., 1998.

[WM] Watson-Marlow. *Peristaltic Pump Drive Units*. Pump.

[WWM12] N. Abdut Aziz S.B. Mohd Noor W.M.F. Wan Mokhtar, F.S. Taip. Process control of pink guava puree pasteurization process: Simulation and validation by experiment. *International Journal on Advanced Science, Engineering and Information Technology*, 2:31–34, 2012.

Appendices

A Matrices hot-water tank and heat exchanger state-space model

The matrices at each operational point for hot-water tank and heat exchanger continuous state-space are:

Operating point 1:

$$A_{cA1} = \begin{pmatrix} -0.001754 & 0 & 0.001595 \\ 0 & -0.91991 & 0 \\ 0.092879 & 0.231010 & -0.244185 \end{pmatrix}$$

$$B_{A1} = \begin{pmatrix} 0 & -0.001356 & 0.000133 \\ -0.001923 & 0 & 0 \\ -0.067769 & 0.128459 & 0 \end{pmatrix}$$

Operating point 2:

$$A_{cA2} = \begin{pmatrix} -0.002818 & 0 & 0.002658 \\ 0 & -0.91991 & 0 \\ 0.193592 & 0.231010 & -0.344898 \end{pmatrix}$$

$$B_{A2} = \begin{pmatrix} 0 & -0.000828 & 0.000133 \\ -0.002824 & 0 & 0 \\ -0.072313 & 0.078405 & 0 \end{pmatrix}$$

Operating point 3:

$$A_{cA3} = \begin{pmatrix} -0.003349 & 0 & 0.003190 \\ 0 & -0.91991 & 0 \\ 0.243949 & 0.231010 & -0.395255 \end{pmatrix}$$

$$B_{A3} = \begin{pmatrix} 0 & -0.000769 & 0.000133 \\ -0.003284 & 0 & 0 \\ -0.081040 & 0.072866 & 0 \end{pmatrix}$$

Operating point 4:

$$A_{cA4} = \begin{pmatrix} -0.003349 & 0 & 0.003190 \\ 0 & -0.91991 & 0 \\ 0.243949 & 0.231010 & -0.395255 \end{pmatrix}$$

$$B_{A4} = \begin{pmatrix} 0 & -0.000942 & 0.000133 \\ -0.003744 & 0 & 0 \\ -0.098564 & 0.089181 & 0 \end{pmatrix}$$

B Matrices holding tube state-space model

The matrices for the discrete holding tube state-space model were:

$$A_B = \begin{pmatrix} 0.9192 & 0 & \cdots & 0 & 0 \\ 1 & 0 & \cdots & 0 & 0 \\ 0 & 1 & \cdots & 0 & 0 \\ \vdots & \vdots & \ddots & \vdots & \vdots \\ 0 & 0 & \cdots & 1 & 0 \end{pmatrix}$$

$$B_{A1} = \begin{pmatrix} 0.2500 \\ 0 \\ \vdots \\ 0 \end{pmatrix}$$

$$B_{A1} = \begin{pmatrix} 0 & \cdots & 0 & 0.3178 \end{pmatrix}$$

C Vertex matrices

The two vertex matrices are:

$$A_1 = \begin{pmatrix} 0.998246 & 0 & 0.001595 \\ 0 & 0.080090 & 0 \\ 0.092879 & 0.231010 & 0.755815 \end{pmatrix}$$

$$A_2 = \begin{pmatrix} 0.996651 & 0 & 0.003190 \\ 0 & 0.080090 & 0 \\ 0.243949 & 0.231010 & 0.604745 \end{pmatrix}$$

D Maple code

Parameters

Parameters **(1)**

$Cp := 4.18 : Ca := 7524 : k1 := 0.4 : k2 := 1.20 : M1 := 82 : M2 := 73.6 : M3 := 49.7 : M4 := 74.5 : Ta := 22 :$

Equations

Equations **(2)**

$$dT2 := \frac{1}{Ca} \cdot (P - k1 \cdot (N2 - 20) \cdot (T2 - (T4 - a)) - k2 \cdot (T2 - Ta))$$

$$\frac{1}{7524} P - 0.00005316321106\ (N2 - 20)\ (T2 - T4 + a) - 0.0001594896332\ T2 + 0.003508771930 \quad \textbf{(3)}$$

$$dTin := \frac{1}{M3 \cdot Cp} \cdot \left(\frac{4.1120 \cdot (N1 - 20) \cdot Cp \cdot (T1 - T3)}{60} - 44 - \frac{4.1120 \cdot (N1 - 20) \cdot Cp \cdot (T3 - b - Ta)}{60} \right)$$

$$0.0003353454059\ (4.1120\ N1 - 82.2400)\ (T1 - T3) - 0.2117970984 - 0.0003353454059\ (4.1120\ N1 - 82.2400)\ (T3 - b - 22) \quad \textbf{(4)}$$

$$dT4 := \frac{2}{M2 \cdot Cp} \cdot \left(\frac{11.1187 \cdot (N2 - 20) \cdot Cp \cdot (T2 - (T4 - a))}{60} - \frac{4.1120 \cdot (N1 - 20) \cdot Cp \cdot (T4 - T3 + b)}{60} - (0.135 \cdot N1 - 0.499) \cdot (T2 - 27) \right) - dTin$$

$$0.0004528985506\ (11.1187\ N2 - 222.3740)\ (T2 - T4 + a) - 0.0004528985506\ (4.1120\ N1 - 82.2400)\ (T4 - T3 + b) - 0.006500936134\ (0.135\ N1 - 0.499)\ (T2 - 27) - 0.0003353454059\ (4.1120\ N1 - 82.2400)\ (T1 - T3) + 0.2117970984 + 0.0003353454059\ (4.1120\ N1 - 82.2400)\ (T3 - b - 22) \quad \textbf{(5)}$$

$$dT3 := \frac{1}{M4 \cdot Cp} \cdot \left(\frac{4.1120 \cdot (N1 - 20) \cdot Cp \cdot (T3 - b - Ta)}{60} + 44 - \frac{4.1120 \cdot (N1 - 20) \cdot Cp \cdot (T1 - T3)}{60} \right)$$

$$0.0002237136465\ (4.1120\ N1 - 82.2400)\ (T3 - b - 22) + 0.1412928293 - 0.0002237136465\ (4.1120\ N1 - 82.2400)\ (T1 - T3) \quad \textbf{(6)}$$

Matriz_A

Matriz_A **(7)**

```
a_T21 := diff(dT2, T2);   a_T22 := diff(dT2, T3);   a_T23 := diff(dT2, T4);
```

$$-0.00005316321106\ N2 + 0.0009037745878 \quad 0 \quad 0.00005316321106\ N2 - 0.001063264221 \quad \textbf{(8)}$$

```
a_T31 := diff(dT3, T2);   a_T32 := diff(dT3, T3);   a_T33 := diff(dT3, T4);
```

$$0 \quad 0.001839821029\ N1 - 0.03679642058 \quad 0 \quad \textbf{(9)}$$

```
a_T41 := diff(dT4, T2);   a_T42 := diff(dT4, T3);   a_T43 := diff(dT4, T4);
```

$$0.005035643115\ N2 - 0.09746889517 - 0.0008776263781\ N1$$

$$0.004620199458\ N1 - 0.09240398916$$

$$-0.005035643115\ N2 + 0.1379592391 - 0.001862318840\ N1 \tag{1}$$

```
A_lin := Matrix([[a_T21, a_T22, a_T23], [a_T31, a_T32, a_T33], [a_T41, a_T42, a_T43]]);
```

$$\left[\left[-0.00005316321106\ N2 + 0.0009037745878,\ 0,\ 0.00005316321106\ N2 - 0.001063264221\right],\right.$$
$$[0,\ 0.001839821029\ N1 - 0.03679642058,\ 0],$$
$$\left.[0.005035643115\ N2 - 0.09746889517 - 0.0008776263781\ N1,\ 0.004620199458\ N1 - 0.09240398916,\ -0.005035643115\ N2 + 0.1379592391 - 0.001862318840\ N1]\right] \tag{2}$$

Matriz_B

$$Matriz\_B \tag{3}$$

```
b_T21 := diff(dT2, N1);   b_T22 := diff(dT2, N2);   b_T23 := diff(dT2, P);
```

$$0$$

$$-0.00005316321106\ T2 + 0.00005316321106\ T4 - 0.00005316321106\ a$$

$$\frac{1}{7524} \tag{4}$$

```
b_T31 := diff(dT3, N1);   b_T32 := diff(dT3, N2);   b_T33 := diff(dT3, P);
```

$$0.001839821029\ T3 - 0.0009199105144\ b - 0.02023803132 - 0.0009199105144\ T1$$

$$0$$

$$0 \tag{5}$$

```
b_T41 := diff(dT4, N1);   b_T42 := diff(dT4, N2);   b_T43 := diff(dT4, P);
```

$$-0.001862318840\ T4 + 0.004620199458\ T3 - 0.003241259149\ b - 0.0008776263781\ T2 - 0.00664077459 - 0.001378940309\ T1$$

$$0.005035643115\ T2 - 0.005035643115\ T4 + 0.005035643115\ a$$

$$0 \tag{6}$$

```
B_lin := Matrix([[b_T21, b_T22, b_T23], [b_T31, b_T32, b_T33], [b_T41, b_T42, b_T43]]);
```

$$\left[\left[0,\ -0.00005316321106\ T2 + 0.00005316321106\ T4 - 0.00005316321106\ a,\ \frac{1}{7524}\right],\right.$$
$$\left[0.001839821029\ T3 - 0.0009199105144\ b - 0.02023803132 - 0.0009199105144\ T1,\ 0,\ 0\right],$$
$$\left.[-0.001862318840\ T4 + 0.004620199458\ T3 - 0.003241259149\ b - 0.0008776263781\ T2 - 0.00664077459 - 0.001378940309\ T1,\ 0.005035643115\ T2 - 0.005035643115\ T4 + 0.005035643115\ a,\ 0]\right] \tag{7}$$